Bulletin of Engineering Geology and the Environment (2023) 82:308
https://doi.org/10.1007/s10064-023-03304-2

ORIGINAL PAPER

Temporal prediction of shallow landslides exploiting soil saturation degree derived by ERA5-Land products

Massimiliano Bordoni[1] · Valerio Vivaldi[1] · Luca Ciabatta[2] · Luca Brocca[2] · Claudia Meisina[1]

Received: 28 July 2022 / Accepted: 5 June 2023 / Published online: 13 July 2023

Abstract

ERA5-Land service has been released recently as an integral and operational component of Copernicus Climate Change Service. Within its set of climatological and atmospheric parameters, it provides soil moisture estimates at different soil depths, represeting an important tool for retrieving saturation degree for predicting natural hazards as shallow landslides. This paper represents an innovative attempt aiming to exploit the use of saturation degree derived from ERA5-Land soil moisture products in a data-driven model to predict the daily probability of occurence of shallow landslides. The study was carried out by investigating a multi-temporal inventory of shallow landslides occurred in Oltrepò Pavese (northern Italy). The achieved results follow: (i) ERA5-Land-derived saturation degree reconstructs well field trends measured in the study area until 1 m from ground; (ii) in agreement with the typical sliding surfaces depth, saturation degree values obtained since ERA5-Land 28–100 cm layer represent a significant predictor for the estimation of temporal probability of occurrence of shallow landslides, able especially to reduce overestimation of triggering events; (iii) saturation degree estimated by ERA5-Land 28–100 cm layer allows to detect soil hydrological conditions leading to triggering in the study area, represented by saturation degree in this layer close to complete saturation. Even if other works of research are required in different geological and geomorphological settings, this study demonstrates that ERA5-Land-derived saturation degree could be implemented to identify triggering conditions and to develop prediction methods of shallow landslides, thanks also to its free availability and constantly updating with a delay of 5 days.

Keywords ERA5-Land · Soil saturation degree · Rainfall · Shallow landslides · Data-driven methods

Introduction

Rainfall-induced shallow landslides are slope instabilities involving the most superficial soil and debris layers, with sliding surfaces typically located between less than 1 to 3 m from ground (Yang et al. 2021). They generally move small volumes of materials (10^1–10^5 m^3), but they can be densely distributed also in little catchments, displacing sediments along hillslopes reaching river network, causing damages to cultivations and infrastructures, contributing to the loss of fertile soils and, sometimes, provoking the loss of human lives (Lacasse et al. 2010). Hence, the development and the implementation of methodologies for their prediction and mitigation represent a pressing need to reduce the negative consequences of these slope instabilities at different scales (Piciullo et al. 2020).

The reconstruction of an effective model for the evaluation of the temporal probability of occurrence of these slope instabilities is a fundamental step for these aims (Guzzetti et al. 2020). These models have the objective to recognize the rainfall conditions which could lead to shallow failures triggering over large areas (Guzzetti et al. 2008). The main approaches that have been adopted to assess the temporal probability of occurrence of shallow landslides are represented by empirical or physically based rainfall thresholds (Brunetti et al. 2010; Ponziani et al. 2012).

Empirical thresholds are reconstructed analyzing the distribution of the rainfall conditions, generally in terms of duration, intensity, and cumulated amounts measured in

✉ Massimiliano Bordoni
massimiliano.bordoni01@universitadipavia.it;
massimiliano.bordoni@unipv.it

[1] Department of Earth and Environmental Sciences, University of Pavia, Via Ferrata 1, 27100 Pavia, Italy

[2] Research Institute for Geo-Hydrological Protection, National Research Council, Via Della Madonna Alta 126, 06128 Perugia, Italy

some field rain gauges, leading to shallow landslide triggering in a test site (Brunetti et al. 2018). The use of easily measurable rainfall data and the reconstruction based on the analysis of real past events make empirical thresholds reliable tools for the estimation of the temporal probability of occurrence of shallow landslides at different scales and different settings (Piciullo et al. 2020). Instead, rainfall thresholds are implemented typically with empirical-statistical approaches (Brunetti et al. 2010) that do not investigate in detail which attributes are the most influencing for the triggering of shallow slope failures in a particular context, especially in terms of antecedent rainfall cumulated amounts (Abraham et al. 2021; Rosi et al. 2021). Furthermore, they do not take into account the effects of hydrological soil conditions, namely soil moisture, saturation degree, soil suction, or pore water pressure, on the rainfall amounts required to trigger shallow landslides (Brocca et al. 2012; Fusco et al. 2019; Conrad et al. 2021).

Physically based thresholds can overcome some of the limits of empirical ones, estimating the triggering rainfall conditions, again in terms of duration, intensity, and cumulated amounts, through the application of deterministic models that can provide the assessment of the link between the rainfall features, the soil hydrological conditions before a rainfall event, and the shear strength response of the soils during the rainwater infiltration (Bordoni et al. 2019; Lee et al. 2021). However, the effectiveness and the spatial representation of those models are limited by the need for a significant amount of geotechnical, mechanical, and hydrological parameters and boundary conditions which are not easy to be measured over large areas and are affected by large heterogeneities (Corominas et al. 2014; Salciarini et al. 2017).

Recently, few attempts have been carried out to develop data-driven models able to estimate the temporal probability of occurrence of rainfall-induced shallow landslides through the identification of the rainfall attributes and soil hydrological parameters which influence more significantly the triggering in a particular test site. Vasu et al. (2016), Park et al. (2019), and Kim et al. (2021) developed data-driven models able to assess the temporal probability of occurrence of rainfall-induced shallow landslides at daily resolution, basing on the cumulative rainfall amount of an event and the antecedent rainfall conditions influencing the occurrence of shallow failures on such a test site. These methods had good effectiveness, but they neglected the soil hydrological conditions present at the beginning of a rainfall event. Observed soil hydrological parameters, namely soil moisture or soil saturation degree, at the beginning of a rainfall event do not correspond only to antecedent rainfall conditions (Brocca et al. 2008), due to the complex subsurface hydrological processes and drainage systems. Especially during concentrated thunderstorms occurring in unsaturated soil conditions, non-equilibrium lags could occur (Mirus et al. 2018; Picarelli et al. 2020). Moreover, the predictability of the water status in soil also depends on the medium-short soil moisture and soil saturation memory characteristics that represent how soil can remind a wet or dry anomaly long after the conditions responsible for the anomaly are forgotten by the atmosphere (Seneviratne et al. 2006; Pan et al. 2019).

Bordoni et al. (2021a) developed a data-driven model which overcame that intrinsic limit of the previous data-driven approach, relating event and antecedent rainfall amounts to soil saturation degree measured at the beginning of a day in the set of the predictors for the temporal probability of occurrence of shallow landslides. This model had a daily resolution, consistently with the minimum temporal discretization able to distinguish triggering events from stable conditions (Piciullo et al. 2020). The developed model was in the frame of the outstanding predictive capability for an 11-year inventory of shallow landslide triggering or not-triggering conditions in the considered test site. Instead, it presented a 5.4% of overestimation, represented by false positives, that are days with modeled unstable conditions even if without real shallow landslides occurrence (205 of 3803 days of the considered time span). For the measure of soil saturation, that model used Advanced SCATterometer (ASCAT) soil moisture datasets characterized by a spatial sampling of 12.5 km and daily temporal resolution (Wagner et al. 2013). These data referred only to the first centimeters of the soil profile, while shallow landslides sliding surfaces are typically located at deeper depths (Mirus et al. 2018). Thus, considering saturation degree at higher depths in a soil profile could be more representative of hydrological conditions leading to shallow landsliding and could limit the number of false positives identified by such a model.

Reanalysis products of soil moisture could provide information to overlap this gap. These datasets are obtained through processes that take all available observations (i.e., field and satellite-based datasets) to calibrate the results of a hydrological model running, whereas an assimilation process refers specifically to adding observation data for correction when the physical model is running (Rodell et al. 2004; Ji et al. 2015; Liu and Yang 2022). In 2019, the European Centre for Medium-Range Weather Forecasts (ECMWF) released the fifth generation of reanalysis data, acknowledged as ECMWF ReAnalysis, ERA5 (Hersbach and Dee 2016; Hersbach et al. 2020). This service was further improved by the release of the ERA5-Land service (Munoz-Sabater et al. 2021) that is now an integral and operational component of the Copernicus Climate Change Service (C3S). Within the set of climatological and atmospheric parameters, ERA5-Land provides global hourly maps of soil moisture from 1950 to present. Soil moisture maps are available for four soil layers, corresponding to 0–7, 7–28, 28–100, and 100–289 cm.

Since the limited time span of availability of these products, only a few attempts exploited ERA5 soil moisture datasets for shallow landslides issues, referring especially to the reconstruction of soil hydrological conditions corresponding to past triggering events (Reder and Rianna 2021) and the development of soil water content-rainfall thresholds (Piciullo and Gilbert 2020; Palazzolo et al. 2022; Uwihirwe et al. 2022). Moreover, thanks to the availability of soil moisture information in depth along the soil profile, the ERA5-Land dataset could provide useful information to improve the reliability of data-driven models of assessment of shallow landslide temporal probability of occurrence, thanks to data related to soil layers that can correspond to sliding surfaces more commonly.

Within this framework, this paper aims to exploit the use of saturation degree values derived from ERA5-Land soil moisture products of different soil layer depths in a data-driven model of the temporal probability of occurrence of shallow landslides at daily resolution. In particular, the following questions would be answered: (i) is ERA5-Land-derived saturation degree a significant predictor of a data-driven model for shallow landslide temporal probability of occurrence? (ii) Which are the improvements in model reliability associated to using ERA5-Land-derived saturation degree of deep soil layers, compared to the values of the most superficial ones? (iii) May ERA5-Land-derived saturation degree estimation be useful to identify the hydrological conditions leading to shallow landslide triggering?

These questions are addressed by investigating a multi-temporal inventory of shallow landslide events that occurred in Oltrepò Pavese (northern Italy).

Materials and methods

The study area

The study area corresponds to the hilly sector of Oltrepò Pavese (265 km^2 wide, Fig. 1a), which represents the northern termination of the Italian Apennines.

The slope altitude ranges between 60 and 500 m a.s.l. According to Koppen's classification, the climatic regime is temperate/mesothermal, with a mean yearly temperature of 12 °C and an average yearly rainfall amount between 700 and 1000 mm, increasing from west to east and from north to south.

From the geological and geomorphological point of view, the northern part of this area is characterized by a lithological bedrock formed by sandstones and conglomerates overlying marls and evaporitic deposits. Superficial soils, derived from bedrock weathering, are mostly clayey or clayey-sandy silts, with a thickness generally less than 2 m. Hillslopes are steep, with an average slope angle between 15° and 20° and values up to 35°, and covered by vineyards, woodlands, and shrublands. The central and southern parts of this present a complex lithological bedrock setting, with calcareous and marlyflyshes, alternated with sandstones, marls, and melanges with block-in-matrix texture. In this area, the soils have clayey or silty clayey texture and thickness of 1.5–2 m or higher where dormant deep slow-moving landslides are present. Also, the geomorphological features of the hillslopes are influenced by bedrock typologies, since they are characterized by a slope angle of 8°–15°.

This area is significantly prone to rainfall-induced shallow landslides (Fig. 1b). Several triggering events have occurred in Oltrepò Pavese since the 1970s (Meisina 2004, 2006) and more than 2500 shallow failures have occurred since 2009 (Bordoni et al. 2021a). Most of these slope instabilities can be classified as complex landslides, starting as roto-translational slides and evolving into flows (Cruden and Varnes 1996). They occur in medium–steep and steep slopes, with a slope angle of at least 8–10°, and are generally 10–500 m long and 10–70 m wide (ratio between length and width of 1.0–7.1) (Bordoni et al. 2021a). These shallow landslides have sliding surfaces which are generally located 90–100 cm from ground. In the study area, this depth corresponds to the contact between soil layers characterized by different physical, mechanical, and hydrological properties. The soil horizons above the sliding surfaces are, in fact, less dense (unit weight, γ, of 16.7–19.0 kN/m^3), more permeable (saturated hydraulic conductivity, K_s, of 10^{-5}/10^{-6} m/s), and less strong (especially due to an effective cohesion, c', of less than 4 kPa) than the layers underlying the sliding surfaces (γ of 18.6–20.3 kN/m^3; K_s of 10^{-7} m/s; c' up to 29 kPa) (Bordoni et al. 2021a, b).

Data

Rainfall measures were collected daily in the period from January 2007 to December 2019 by a network of 21 rain gauges (blue circles in Fig. 1c). These datasets were used to retrieve the considered rainfall cumulative amount predictors of the model for the temporal probability of occurrence (Table 1).

Saturation degree datasets, in correspondence with each considered rain gauge, were obtained through different sources (Table 1).

As in the data-driven method for the assessment of the temporal probability of occurrence proposed by Bordoni et al. (2021a), saturation degree predictors were retrieved from datasets collected by the Advanced SCATterometer (ASCAT) sensor onboard the Metop satellites. ASCAT is a C-band (5.255 GHz) instrument characterized by a spatial resolution of 12.5 km and a daily temporal resolution (Wagner et al. 2013). The retrieval algorithm is based on a change detection technique and allows estimation of the saturation

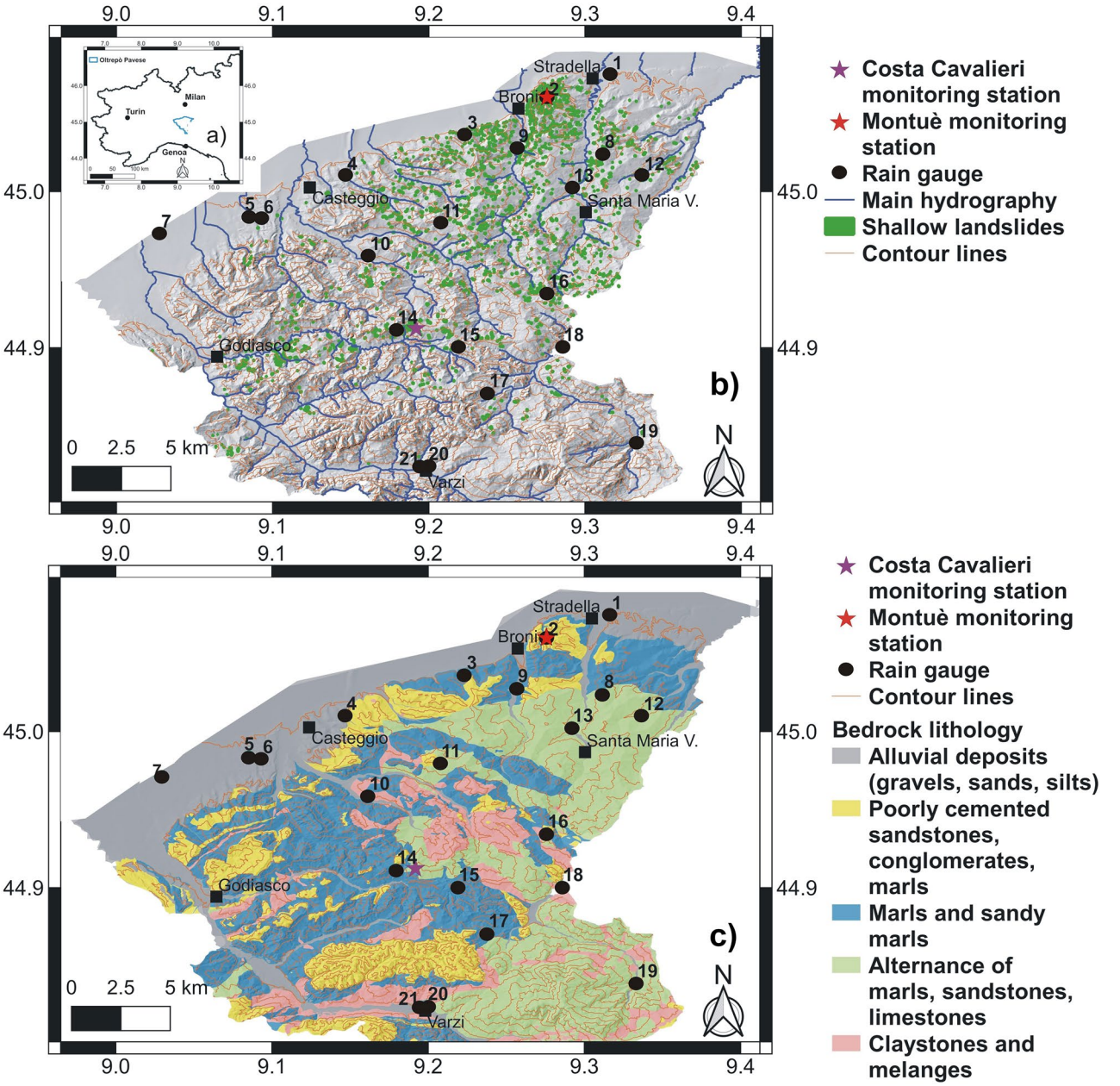

Fig. 1 The study area: **a** location; **b** shallow landslides distribution; **c** bedrock lithological map

degree only of the first centimeters of soil (< 0.1 m in depth). In this study, the products provided within the EUMETSAT project H SAF (http://hsaf.meteoam.it/) denoted as H115 have been used.

Saturation degree predictors also corresponded to datasets acquired from ERA5-Land soil moisture products (Munoz-Sabater et al. 2021). ERA5-Land is a reanalysis data service released by ECMWF which produces 50 variables describing the water and energy cycles over land, globally, at hourly temporal resolution and with a spatial resolution of 9 km, matching the ECMWF triangular-cubic-octahedral (TCo1279) operational grid (Malardel et al. 2016). Within this set of variables, ERA5-Land provides maps of soil moisture for four soil layers, namely 0–7, 7–28, 28–100, and 100–289 cm from ground level. In this study, ERA5-Land soil moisture data of all these four soil layers measured at 0:00 UTC were retrieved for the analyzed periods. The saturation degree was then estimated for each soil layer as the ratio between the measured soil moisture θ and the saturated water content θ_s, corresponding to the highest soil moisture measured along the time span for each soil layer.

Table 1 Predictors of the data-driven model

Predictor	Data source, resolution, and depth of measure	Influence on shallow landslides occurrence
Daily rainfall amount (1-day rainfall) Cumulated rainfall of 3 days (3-day rainfall) Cumulated rainfall of 5 days (5-day rainfall) Cumulated rainfall of 7 days (7-day rainfall) Cumulated rainfall of 10 days (10-day rainfall) Cumulated rainfall of 15 days (15-day rainfall) Cumulated rainfall of 30 days (30-day rainfall) Cumulated rainfall of 45 days (45-day rainfall) Cumulated rainfall of 60 days (60-day rainfall)	Rain gauge networks with daily resolution, measuring at ground level	They represent the effects of intense daily rainfall amount and/or antecedent rainfall amounts on the increase in soil saturation degree and on the consequent decrease in soil shear strength, which could lead to shallow landslide triggering (Aleotti 2004; Giannecchini et al. 2012; Zezere et al. 2015; Guzzetti et al. 2020)
Saturation degree at the beginning of a certain day (SAT)	ASCAT sensor with spatial resolution of 12.5 km, which allows us to estimate saturation degree of the first centimeters of soil (< 0.1 m in depth) ERA5-Land products with spatial resolution of 9 km, which allow us to estimate saturation degree of four soil layers: 0–7, 7–28, 28–100, 100–289 cm in depth	They represent the differences in rainwater infiltration and in the other hydrological processes that occur in soils with different saturation degree levels, when similar rainfall events affect an area (Lu and Godt 2013; Leonarduzzi et al. 2021)

The response variable of all the models was represented by a multi-temporal shallow landslide inventory reconstructed from January 2007 to December 2018. Another multi-temporal inventory covering January–December 2019 was used for the external validation of the best models. Both inventories were reconstructed at the daily resolution, indicating shallow landslides' triggering and not-triggering days. The triggering days on these inventories were obtained from reports of public administrations, newspapers, and online chronicles (Bordoni et al. 2021a). Shallow landslides were triggered in 212 days of the 2007–2018 inventory. At the same time, shallow failures occurred in 10 days of the 2019 inventory.

Comparison between field, ASCAT, and ERA5-Land trends of saturation degree

A preliminary evaluation of the reliability of saturation degree estimated by ASCAT and ERA5-Land products is required for their use as predictors of the temporal occurrence of shallow slope instabilities and for identifying the main hydrological conditions leading to their triggering.

ASCAT and ERA5-Land saturation degree trends were compared with field-measured trends in correspondence of two monitoring stations (Montuè and Costa Cavalieri, star symbols in Fig. 1c) located in the Oltrepò Pavese area.

These two test sites are representative of the main geological and geomorphological settings of Oltrepò Pavese prone to shallow landsliding: steep slopes (> 20°) covered by shrubs and grasses or woodlands of black robust trees with clayey silts, as at Montuè; medium–steep slopes (8–15°) covered by sowed fields (e.g., wheat, alfalfa) with silty clays, as at Costa Cavalieri.

The soil profiles of these test sites represent the materials typically involved in shallow landslides in the study area. These soils' main physical, mechanical, and hydrological properties are listed in Tables 2 and 3. Furthermore, Fig. 2 shows the water retention curves of the different soil layers.

At the Montuè test site, the soil is characterized by a homogeneous clayey-sandy silt texture, with low plasticity and a high amount (> 15%) of carbonate content as soft concretions. Along this profile, the most superficial layer, generally until about 1 m from ground level, is characterized by a γ of 16.7–18.6 kN/m^3, high friction angle (φ'; 31–33°), and nil c'. This layer is also permeable, with K_s around 10^{-5}/10^{-6} m/s, and with low water retention, as testified by values of Van Genucthen's (1980) model of water retention curve parameters of 0.003–0.012 kPa^{-1} and 1.38–1.57 for α and n, respectively. The soil layers below 1 m from ground level, underlying also the typical sliding surfaces depth of shallow landslides, have higher γ (18.2–18.6 kN/m^3) and c' (29 kPa), but they are less permeable (K_s of 10^{-7} m/s) and with higher water retention (0.013 kPa^{-1} and 1.19 for α and n, respectively). Along the soil profile, saturated water content (θ_s) and residual water content (θ_r) keep in a narrow range, especially below 20 cm from ground level (0.37–0.44 and 0.01 m^3/m^3 for θ_s and θ_r, respectively).

At Costa Cavalieri, the soil is characterized by a homogeneous silty clay texture, with high plasticity and medium–high amount (> 10%) of carbonate content as soft concretions. Along this profile, the most superficial layers, generally until about 1 m from ground level, are characterized by γ of 18.6–19.0 kN/m^3, low φ' (10°), and nil c'.

Table 2 Main hydrological properties of the test site soils

Depth of measure-field (cm)	Depth of measure-ERA5-Land (cm)	θ_s-field (m^3/m^3)	θ_s-ERA5-Land (m^3/m^3)	θ_r (m^3/m^3)	α (kPa^{-1})	n (-)	K_s (m/s)
Montuè							
20	7–28	0.32–0.33	0.42	0.02	0.003	1.57	10^{-5}
60	28–100	0.37–0.40	0.42	0.01	0.012	1.38	10^{-6}
100	28–100	0.37–0.40	0.42	0.01	0.012	1.38	10^{-6}
120	100–289	0.40–0.44	0.42	0.01	0.013	1.19	10^{-7}
Costa Cavalieri							
20	7–28	0.41–0.49	0.45	0.01	0.007	1.30	10^{-5}
60	28–100	0.43–0.51	0.45	0.01	0.017	1.30	10^{-5}
90	28–100	0.45–0.51	0.45	0.01	0.017	1.30	10^{-5}
170	100–289	0.45–0.47	0.45	0.01	0.005	1.21	10^{-7}

θ_s-field is the saturated water content measured in field; θ_s-ERA5-Land is the saturated water content measured through ERA5-Land; θ_r, α, and n are residual water content and the fitting parameters of Van Genuchten's (1980) model of water retention curve, respectively, estimated in laboratory through an evaporation technique from undisturbed soil samples; K_s is the saturated hydraulic conductivity, measured in the field through an amoozometer

Table 3 Main physical and mechanical properties of the test site soils

Depth of measure-field (cm)	Depth of measure-ERA5-Land (cm)	γ (kN/m^3)	φ' (°)	c' (kPa)
Montuè				
20	7–28	16.7–17.0	31	0.0
60	28–100	17.0–18.6	33	0.0
100	28–100	17.0–18.6	33	0.0
120	100–289	18.2–18.6	26	29.0
Costa Cavalieri				
20	7–28	18.7–19.0	10	0.0
60	28–100	18.6–19.0	10	0.0
90	28–100	18.6–19.0	10	0.0
170	100–289	19.3–20.3	18	0.0

γ is the unit weight of soil, measured in laboratory from undisturbed soil samples; φ' and c' are the peak friction angle and the soil effective cohesion, respectively, measured in laboratory from undisturbed soil samples through direct shear tests

This layer has K_s around 10^{-5} m/s and low water retention (0.007–0.017 kPa^{-1} and 1.30 for α and n, respectively). The soil layers below 1 m from ground level, underlying also the typical sliding surfaces depth of shallow landslides, have higher γ (19.3–20.3 kN/m^3) and φ' (18°), but they are less permeable (K_s of 10^{-7} m/s) and with higher water retention (0.005 kPa^{-1} and 1.21 for α and n, respectively). Along the soil profile, saturated water content (θ_s) and residual water content (θ_r) keep in a narrow range, especially below 20 cm from ground level (0.43–0.51 and 0.01 m^3/m^3 for θ_s and θ_r, respectively).

In the test sites, sensors for the measurement of soil water content, namely time-domain reflectometer probes (CS610, Campbell Sci. Inc., Logan, UT) at Montuè and frequency-domain reflectometer probes (GS3, Decagon Devices Inc., Pullman, WA) at Costa Cavalieri, have been installed at different depths and have been collecting data since March 2012 and December 2015 at Montuè and Costa Cavalieri, respectively (Bordoni et al. 2021b) (Fig. 3). Daily trends of soil water content acquired by these probes were transformed in daily saturation degree trends, as the ratio between the measured soil moisture θ and θ_s estimated in the field as the highest value of soil moisture measured along the monitored time span for each soil layer (Bordoni et al. 2021b) (Table 2).

At both the test sites (Fig. 3), saturation degree trends of ASCAT, ERA5-Land 0–7 cm layer and ERA5-Land 7–28 cm were compared each other and with the most superficial monitored field trends of soil saturation degree, corresponding to the depth of 20 cm from the ground at both the test sites. The saturation degree trend of the ERA5-Land 28–100 cm layer was compared with field trends collected at depths located within this range, which corresponded to 90–100 cm from ground level at both test sites. Moreover, the saturation degree trend of the ERA5-Land 100–289 cm layer was compared with field trends collected at depths located within this range, which were 120 and 170 cm at Montuè and Costa Cavalieri, respectively. The comparisons were made between November 2012–December 2019 and March 2016–December 2019 at Montuè and Costa Cavalieri, respectively.

The performance metrics used for the comparison between ASCAT, ERA-5 Land, and field-measured saturation degree were the bias and the correlation coefficient (r). Bias and r represent the mean systematic difference

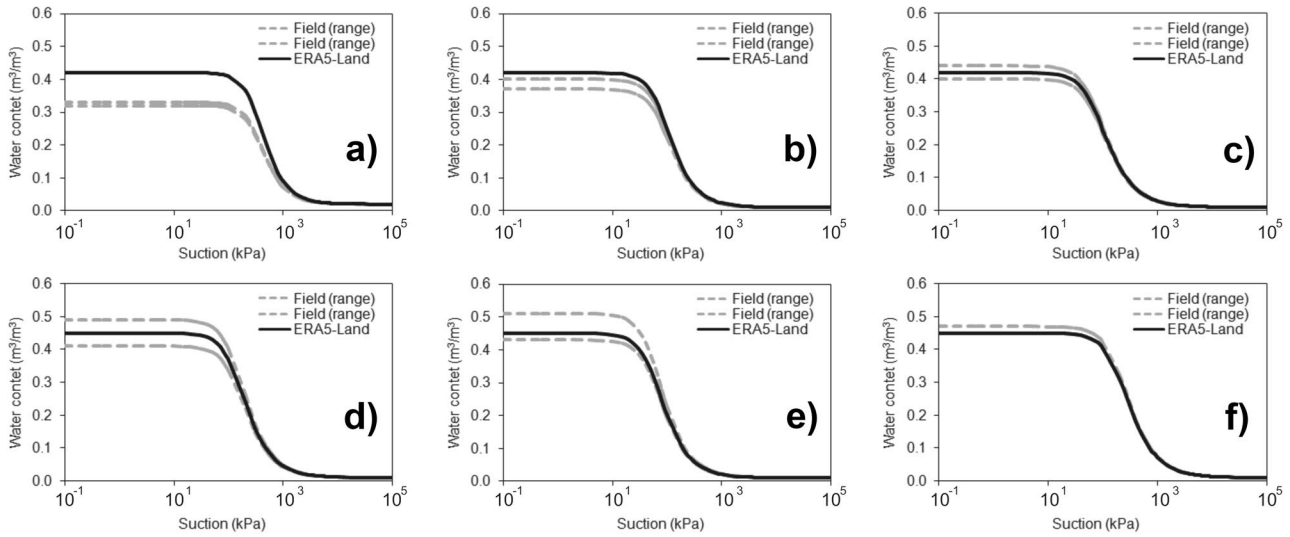

Fig. 2 Water retention curves of the analyzed soil layers: **a** ERA5-Land layer of 7–28 cm at Montuè; **b** ERA5-Land layer of 28–100 cm at Montuè; **c** ERA5-Land layer of 100–289 cm at Montuè; **d** ERA5-Land layer of 7–28 cm at Costa Cavalieri; **e** ERA5-Land layer of 28–100 cm at Costa Cavalieri; **f** ERA5-Land layer of 100–289 cm at Costa Cavalieri

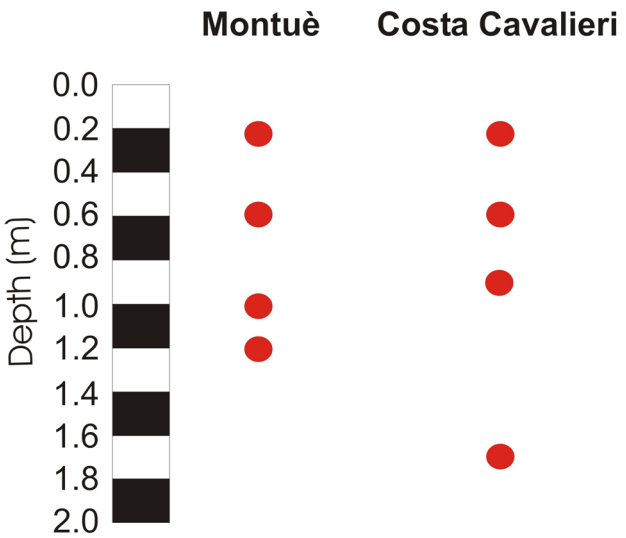

Fig. 3 Distribution of the probes for water content monitoring in field (red circles) along the two tested soils

and the temporal variation consistency between two trends of the same parameter, respectively (Wu et al. 2021).

A data-driven method for the assessment of the temporal probability of occurrence of shallow landslides

The flowchart of the methodological approach developed for estimating the temporal probability of the occurrence of shallow landslides is shown in Fig. 4. The method was refined from the one first proposed by Bordoni et al. (2021a, b) and is based on the assumption that shallow failures triggering occur as a consequence of significant rainfall amounts coupled with particular soil hydrological conditions related in particular to a high degree of saturation in soil layers (Lu and Godt 2013). According to this, the model considered the following potential predictors (Table 1): (i) the rainfall amount of one day; (ii) the cumulative rainfall amounts in different periods (3, 5, 7, 10, 15, 30, 45, 60 days);(iii) the soil saturation degree measured at 0:00 UTC of a particular day. Concerning the cumulative rainfall amounts, the most adopted parameters considered in previous works (Aleotti 2004; Giannecchini et al. 2012; Tien Bui et al. 2013; Vasu et al. 2016; Kim et al. 2020) to build models of temporal assessment of the occurrence of shallow landslides were considered. The soil saturation degree represents the soil hydrological conditions present at the beginning of a certain day to represent the differences in rainwater infiltration and in the other hydrological processes that occur in soils with different saturation degree levels when similar rainfall events affect an area (Lu and Godt 2013; Leonarduzzi et al. 2021).

The response variable of the model was the database of January 2007–December 2018, indicating the days when at least one shallow failure occurred or no phenomena were triggered in a circular buffer of 10 km of radius centered from each rain gauge used for the measure of rainfall amounts. The buffer dimension was selected according to the morphology and the density of rain gauges in the study area (Bordoni et al. 2021a). The indications of landslide triggering were then transformed into a binary response variable,

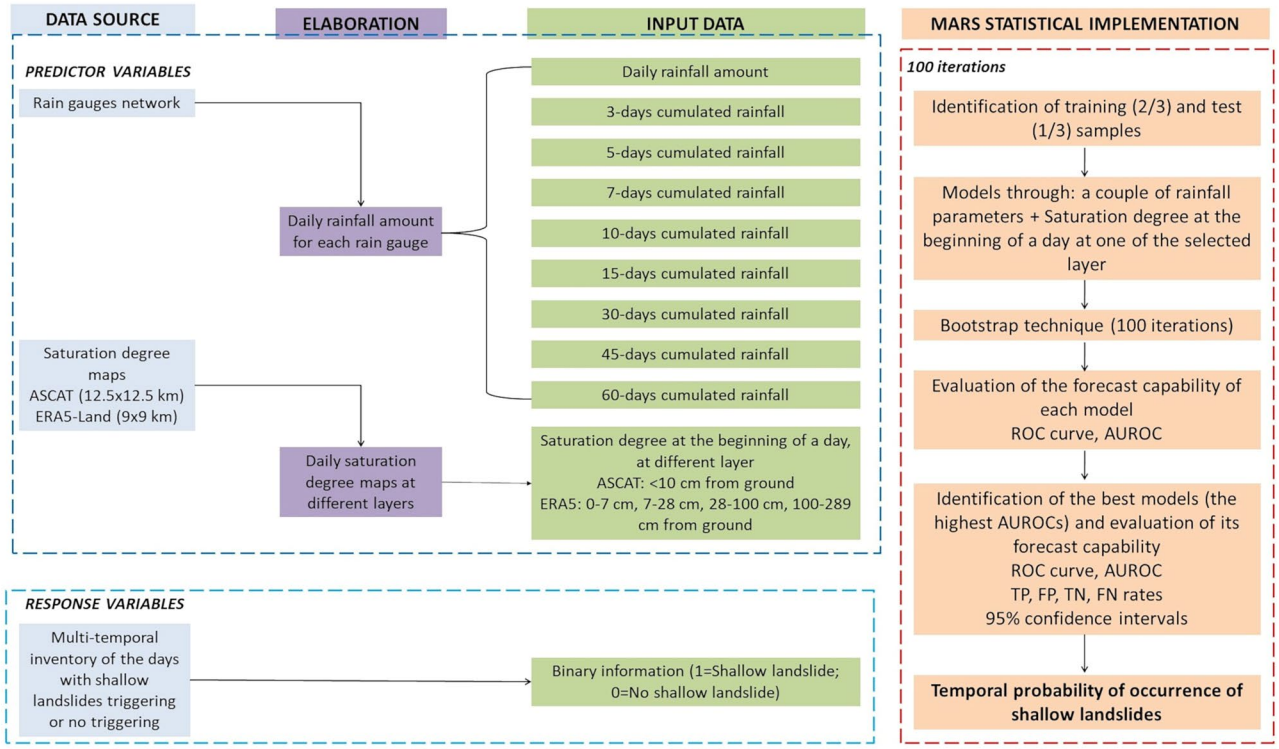

Fig. 4 Flowchart of the developed data-driven model

assigning 0 or 1 in case of landslide absence or presence, respectively.

The predictors and the response variable were merged in a matrix to apply the data-driven methodology. Models based on Multivariate Adaptive Regression Splines (MARS) technique (Friedman 1991) were built, each considering several rainfall predictors and the saturation degree. Each model was reconstructed by a database, formed by all triggering days and the same number of days without triggering and then subdivided into a training set (2/3 of this dataset) and a test set (the remaining 1/3 of the dataset). Training and test selection were repeated for each model in a 100-fold bootstrap procedure to create 100 fitted bootstrap scenarios to extend the prediction to the entire database. The mean value and confidence interval of each bootstrap distribution of 100 probability values were calculated to obtain the temporal probability of occurrence for each dataset day. The reliability of each model was then estimated by calculating the mean value of the 100 area under the receiver operating characteristic (ROC) curve (AUROC; Hosmer and Lemeshow 2000) obtained from the 100-fold bootstrap procedure.

Because of the availability of different saturation degree products, in this study, the effect of these products on the model's predictive capability was analyzed through the reconstruction of data-driven models considering the saturation degree derived by one product each time. Thus, five different sets of data-driven models were built, considering: (i) soil saturation degree derived by ASCAT; (ii) soil saturation degree of 0–7 cm layer of ERA5-Land; (iii) soil saturation degree of 7–28 cm layer of ERA5-Land; (iv) soil saturation degree of 28–100 cm layer of ERA5-Land; (v) soil saturation degree parameters of 100–289 cm layer of ERA5-Land.

The best model within each set was identified as the one with the highest AUROC. For the selected best models, a 2×2 a posteriori contingency table was reconstructed, considering 0.5 as the threshold to discriminate days with limited possibility of shallow landslide triggering (temporal probability of occurrence ≤ 0.75) from days with a significant probability of shallow landslides occurrence (temporal probability of occurrence > 0.75). In this way, for those models, their performance was also evaluated through the indexes of true positives (TP), false positives (FP), true negatives (TN), and false negatives (FN) (Galanti et al. 2018).

Validation of the data-driven models

External validation was also carried out to verify the reliability of the best models reconstructed through the data-driven methodology. This corroboration was done considering different multi-temporal datasets than the one used for reconstructing the models. They corresponded to the datasets of

the triggering and not-triggering days that occurred between January and December 2019 close to Montuè and Costa Cavalieri test sites (star symbols in Fig. 1). The reliability of the selected models was evaluated through the same statistical approach, and the same four indexes (TP, FP, TN, FN) used for the assessment of the predictive capability of the same models considering 2007–2018 multi-temporal inventory.

Identification of hydrological conditions leading to shallow landslide triggering

Once identified the best model for the assessment of the temporal probability of occurrence of shallow landslides was, the estimated values of saturation degree of the product used in the best model were compared to the real measured conditions of saturation degree at the beginning of triggering days monitored in the field during November 2012–December 2019 and March 2016–December 2019 at Montuè and Costa Cavalieri, respectively. The field values of saturation degree used for this comparison were the ones measured in correspondence with the typical sliding surface depth of shallow landslides in the study area, which corresponded to 0.9–1.0 from ground level (Bordoni et al. 2021a, b).

Results

Comparison between field, ASCAT, and ERA5-Land trends of saturation degree at different depths

The performance indexes adopted to verify the similarity between ERA5-Land and field trends indicated a good level of correspondence, demonstrated by r of 0.77–0.88 and bias of 0.08–0.14 for the soil layers until 0.6 m from the ground, which decreased at 0.9–1.0 m from ground (r of 0.80–0.83, the bias of 0.09–0.11). Instead, the saturation degree trend derived by ERA5-Land 100–289 cm layer was not significantly similar to the field trends measured at 1.2 m from the ground in Montuè ($r = 0.62$, bias = 0.22) and 1.7 m from the ground in Costa Cavalieri ($r = 0.60$, bias = 0.19).

The high values of these statistical indexes indicate that ERA5-Land trends are in good agreement with the field-measured temporal trends of saturation degree up to 0.9–1.0 m from the ground of both test sites, identifying the variation of soil hydrological behaviors throughout the different seasons and concerning dry and wet periods (Figs. 5 and 6).

Saturation degree dynamics showed dry phases when soils experienced values of saturation degree lower than 0.5, corresponding to values of suction in the order of 300–1000 kPa (Bordoni et al. 2021b). Dry periods were alternated with wet time spans, when the saturation degree was close to 1, representing complete saturation of a soil layer and nil suction (Bordoni et al. 2021b). In both the test sites, the lowest values of saturation degree were typical in the months between June and September. In these periods, fast increases of soil saturation, until about 0.8–0.9, could occur in correspondence with thunderstorms or rainfall events, causing also a decrease in soil suction until 10 kPa (Bordoni et al 2021b). These events were followed by a rapid decrease in soil saturation for infiltration and evapotranspiration effects. During these conditions, the fast drainage of rainwater in the most shallow soil horizons can also be caused by the presence of macro-voids and desiccation cracks, especially in the silty clays of Costa Cavalieri (Bordoni et al. 2021b). Re-wetting during the beginning of autumn (end of September–first half of October) was also fast and was measured by both field and ERA5-Land datasets. Re-wetting occurred from the most superficial soil layers to the deepest ones at about 100 cm from the ground until the soil saturation degree kept with typical values higher than 0.8 (suction values below 100 kPa; Bordoni et al. 2021b) and could further increase in correspondence of intense and/or prolonged rainy periods, when soil layers could approach or get conditions close to 1 in saturation degree and close to 0 kPa in terms of soil suction. During these rainfall events, complete saturation of these soil layers developed through a mechanism of upraising of a transient water table, from the bottom to the most shallow horizons, that developed since the contact at about 1 m from the ground between soil horizons with different hydrological and physical features (soil layers until 1 m with high permeability and low unit weight; soil layers below 1 m with lower permeability and higher unit weight). Both field and ERA5-Land datasets could detect these dynamics at different depths along the soil profiles of both the considered sites.

Both test sites' deepest monitored soil layers, located at 1.2 and 1.7 m in Montuè and Costa Cavalieri, respectively, were characterized by a different hydrological behavior (Figs. 5f and 6f). Dry conditions in summer and autumn, with saturation lower than 0.6 (suction values higher than 1000 kPa; Bordoni et al. 2021b), were alternated with periods of saturation higher than 0.9 (soil suction lower than 100 kPa; Bordoni et al. 2021b), typical of winter and spring months that were not reached during all the monitored years. The increase in saturation degree of the layers below 1 m from the ground was due to the rainwater infiltration from the most superficial layers, which occurred more slowly than in the most superficial horizons for the lower permeability and the higher unit weight. This different dynamic, also related to the deepest position of these layers in the soil profiles, was not completely caught by the saturation degree trends reconstructed since the ERA5-Land 100–289 cm layer dataset, which were smoother and kept higher of 0.1–0.3 in saturation than the measured ones during dry periods in summer and autumn months. Furthermore, not all the

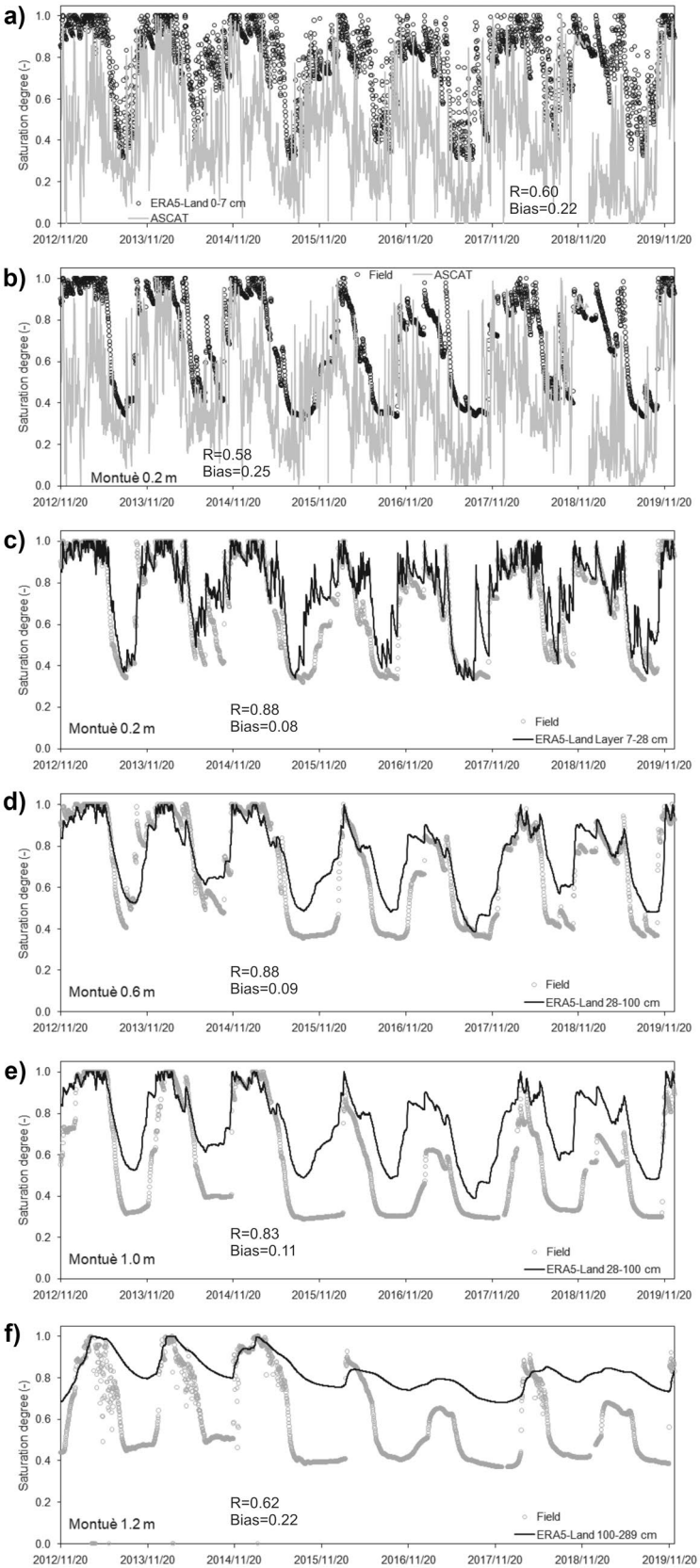

Fig. 5 Comparison between field-monitored and ERA5-Land or ASCAT-derived saturation degree for Montuè test site: **a** ERA5-Land 0–7 cm and ASCAT; **b** field and ASCAT at 0.2 m; **c** field and ERA5-Land 7–28 cm at 0.2 m; **d** field and ERA5-Land 28–100 cm at 0.6 m; **e** field and ERA5-Land 28–100 cm at 1.0 m; **f** field and ERA5-Land 100–289 cm at 1.2 m

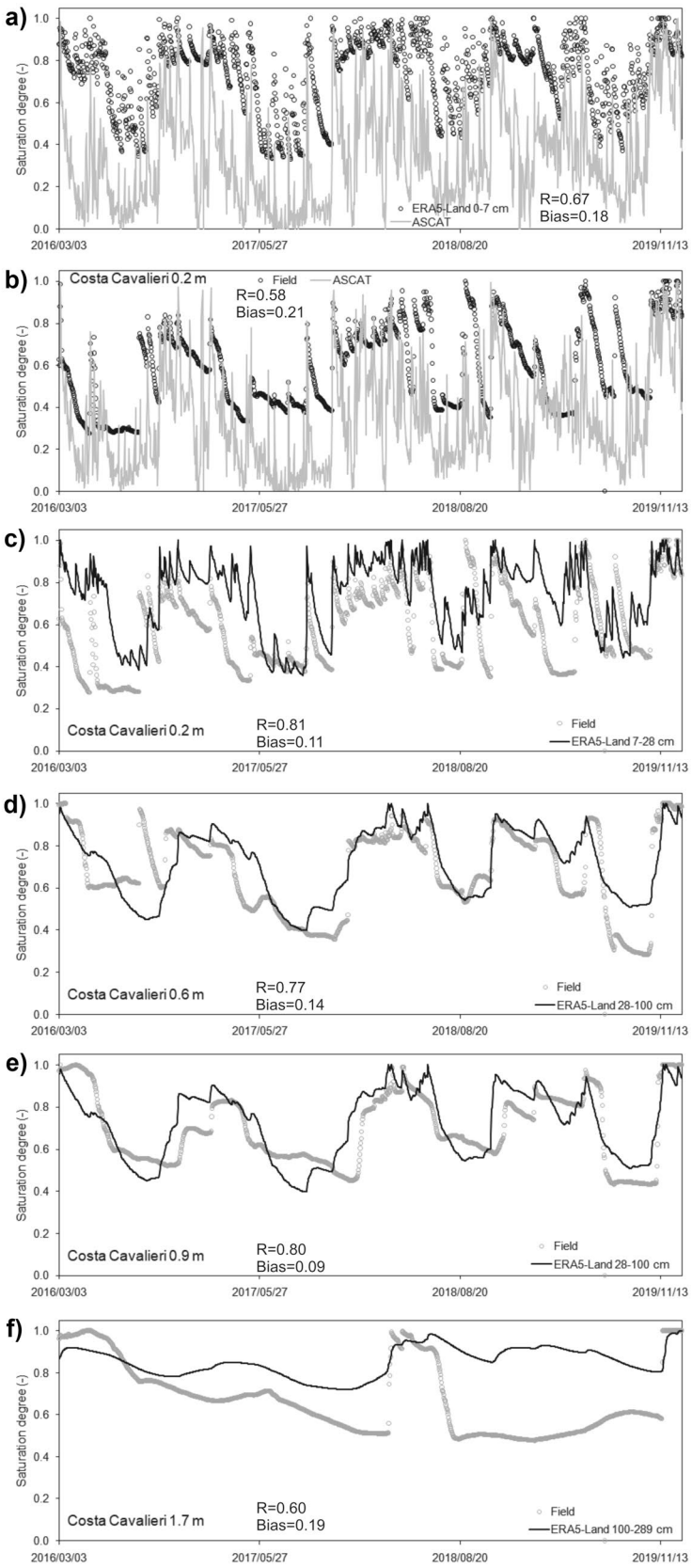

Fig. 6 Comparison between field-monitored and ERA5-Land or ASCAT-derived saturation degree for Costa Cavalieri test site: **a** ERA5-Land 0–7 cm and ASCAT; **b** field and ASCAT at 0.2 m; **c** field and ERA5-Land 7–28 cm at 0.2 m; **d** field and ERA5-Land 28–100 cm at 0.6 m; **e** field and ERA5-Land 28–100 cm at 0.9 m; **f** field and ERA5-Land 100–289 cm at 1.7 m

periods with field measures of saturation degree close to 1 were correctly identified by ERA5-Land 100–289 cm layer dataset from 30 November–31 December 2019 in Montuè and from 1 March–19 May 2016 in Costa Cavalieri.

As regards the reliability of ASCAT products, the saturation degree trends were reconstructed since this dataset had a limited correspondence to the corresponding ERA5-Land 0–7 cm layer dataset ($r = 0.60$–0.67, bias = 0.18–0.22; Figs. 5a and 6a). Even if ASCAT trends of saturation degree followed the hydrological behaviors measured by ERA5-Land 0–7 cm layer dataset and characterized by alternate between periods of low level in soil saturation (saturation < 0.5) and time spans with conditions close to complete saturation (saturation > 0.9), ASCAT trends were more scattered, with also some days when measures kept lower than 0.3. Moreover, ASCAT saturation degree trends showed a limited correspondence ($r = 0.58$, bias = 0.21–0.25) with the most shallow soil level monitored in the field, corresponding to 0.2 m from the ground at both Montuè and Costa Cavalieri (Figs. 5b and 6b).

Models of the temporal probability of occurrence of shallow landslides

For each available saturation degree dataset of ASCAT and ERA-5 Land, the best models for estimating the temporal probability of occurrence of shallow landslides were reconstructed in terms of AUROC (Tables 4, 5, 6, 7, and 8). Considering the ASCAT dataset, the best model was the one that considered the cumulated rainfall amount of 3 (3-day rainfall) and 30 days (30-day rainfall), together with the soil saturation degree measured by the ASCAT satellite at the beginning of an event. Considering ERA5-Land datasets, the best models considered different rainfall

Table 4 AUROC of models reconstructed using ASCAT saturation degree

	1-day rainfall	3-days rainfall	5-days rainfall	7-days rainfall	15-days rainfall	20-days rainfall	30-days rainfall	45-days rainfall	60-days rainfall
1-day rainfall		0.96	0.96	0.94	0.94	0.92	0.91	0.90	0.90
3-days rainfall			0.96	0.96	0.96	0.96	**0.97**	0.91	0.88
5-days rainfall				0.94	0.89	0.89	0.89	0.88	0.90
7-days rainfall					0.85	0.90	0.82	0.90	0.88
15-days rainfall						0.88	0.84	0.82	0.85
20-days rainfall							0.84	0.83	0.83
30-days rainfall								0.85	0.83
45-days rainfall									0.82
60-days rainfall									

Table 5 AUROC of models reconstructed using ERA5-Land 0–7 cm saturation degree

	1-day rainfall	3-days rainfall	5-days rainfall	7-days rainfall	15-days rainfall	20-days rainfall	30-days rainfall	45-days rainfall	60-days rainfall
1-day rainfall		0.96	0.96	0.96	0.96	0.96	0.92	0.85	0.85
3-days rainfall			0.96	0.96	0.96	0.96	**0.97**	0.93	0.90
5-days rainfall				0.92	0.92	0.90	0.90	0.87	0.86
7-days rainfall					0.90	0.90	0.91	0.90	0.90
15-days rainfall						0.83	0.82	0.82	0.81
20-days rainfall							0.85	0.85	0.84
30-days rainfall								0.85	0.85
45-days rainfall									0.85
60-days rainfall									

Table 6 AUROC of models reconstructed using ERA5-Land 7–28 cm saturation degree

	1-day rainfall	3-days rainfall	5-days rainfall	7-days rainfall	15-days rainfall	20-days rainfall	30-days rainfall	45-days rainfall	60-days rainfall
1-day rainfall		0.94	**0.97**	0.96	0.96	0.95	0.95	0.89	0.89
3-days rainfall			0.95	0.96	0.96	0.96	0.96	0.95	0.93
5-days rainfall				0.96	0.96	0.96	0.96	0.95	0.93
7-days rainfall					0.92	0.92	0.92	0.92	0.91
15-days rainfall						0.94	0.94	0.95	0.93
20-days rainfall							0.92	0.92	0.92
30-days rainfall								0.92	0.90
45-days rainfall									0.90
60-days rainfall									

Table 7 AUROC of models reconstructed using ERA5-Land 28–100 cm saturation degree

	1-day rainfall	3-days rainfall	5-days rainfall	7-days rainfall	15-days rainfall	20-days rainfall	30-days rainfall	45-days rainfall	60-days rainfall
1-day rainfall		0.96	0.97	0.96	0.94	0.94	0.92	0.89	0.89
3-days rainfall			0.96	**0.98**	0.95	0.94	0.93	0.93	0.93
5-days rainfall				0.95	0.94	0.94	0.92	0.95	0.93
7-days rainfall					0.92	0.92	0.92	0.92	0.91
15-days rainfall						0.94	0.94	0.95	0.93
20-days rainfall							0.92	0.92	0.92
30-days rainfall								0.92	0.90
45-days rainfall									0.90
60-days rainfall									

Table 8 AUROC of models reconstructed using ERA5-Land 100–289 cm saturation degree

	1-day rainfall	3-days rainfall	5-days rainfall	7-days rainfall	15-days rainfall	20-days rainfall	30-days rainfall	45-days rainfall	60-days rainfall
1-day rainfall		0.83	0.85	0.84	0.86	0.83	0.86	0.88	0.88
3-days rainfall			0.85	0.86	0.85	0.86	0.86	0.88	0.88
5-days rainfall				0.86	0.85	0.85	0.88	0.89	0.89
7-days rainfall					0.90	0.89	**0.91**	0.90	0.88
15-days rainfall						0.90	0.88	0.88	0.88
20-days rainfall							0.87	0.87	0.88
30-days rainfall								0.85	0.84
45-days rainfall									0.83
60-days rainfall									

predictors, together with the selected dataset of saturation degree: 3-day rainfall and 30-day rainfall considering the ERA5-Land 0–7 cm layer; 1-day rainfall and 5-day rainfall considering the ERA5-Land 7–28 cm layer; 3-day rainfall and 7-day rainfall considering the ERA5-Land 28–100 cm layer; and 7-day rainfall and 30-day rainfall considering the ERA5-Land 100–289 cm layer.

Even if all the best models were characterized by outstanding performance, testified by average AUROC values between 0.91 and 0.98 (Fig. 7a), their predictive capabilities were discriminated according to the values of TP, TN, FP, and FN indexes. All these models effectively recognized the daily occurrence of shallow landslides in the considered input inventory, as confirmed by TP of 96.2–97.2% and FN of 2.8–3.8% (Fig. 7b, c). In terms of days, all these models were able to estimate correctly 204–206 of the 212 triggering days reported in the input inventory (Fig. 8a).

However, the overestimation of the models, represented by the calculated values of TN and FP, was different. In these terms, the most reliable model was the one that considered ERA5-Land 28–100 cm layer saturation degree together with 3 days of rainfall and 7 days of rainfall, which had

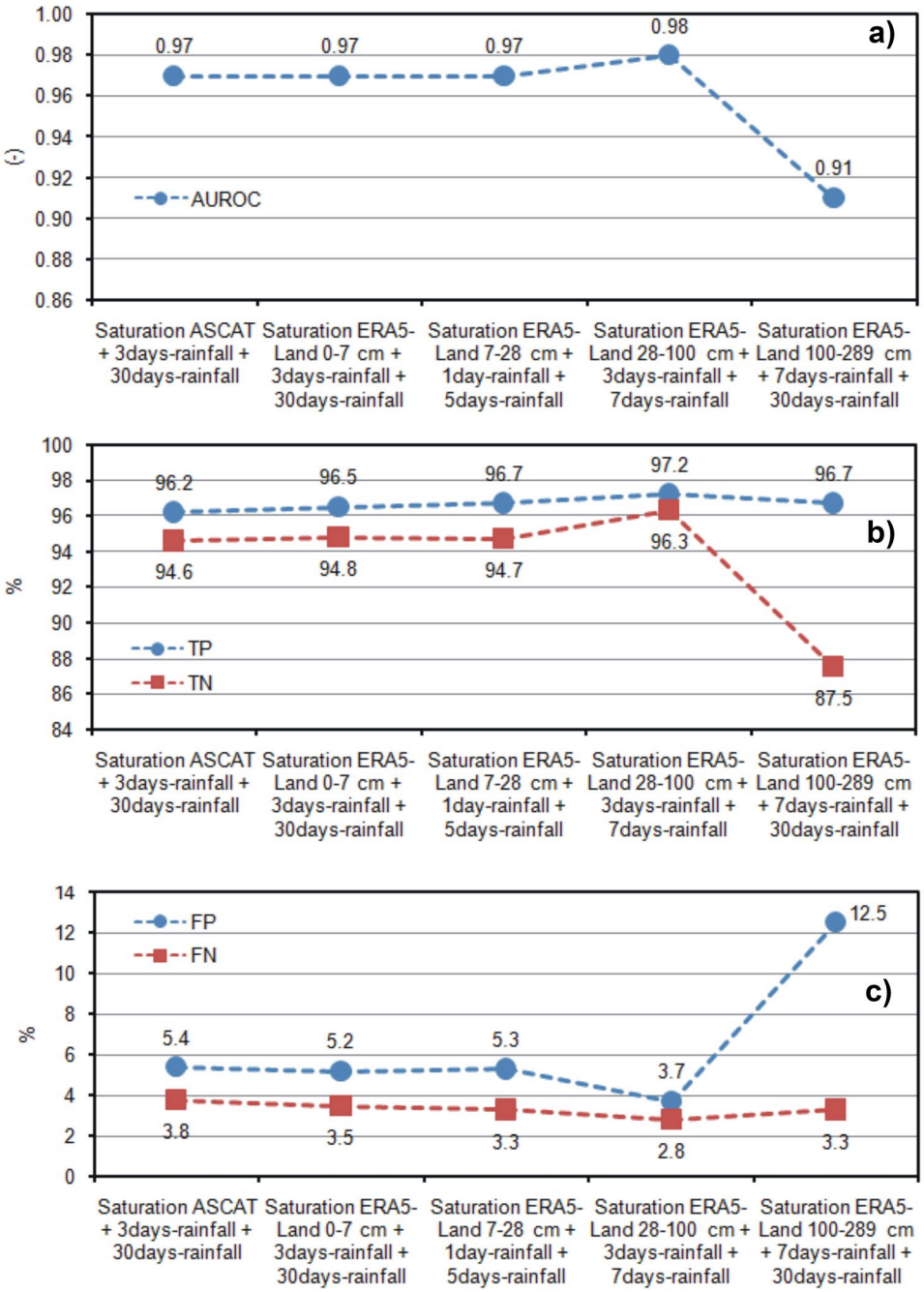

Fig. 7 AUROC (**a**), TP-TN (**b**), and FP-FN (**c**) of the best-reconstructed models

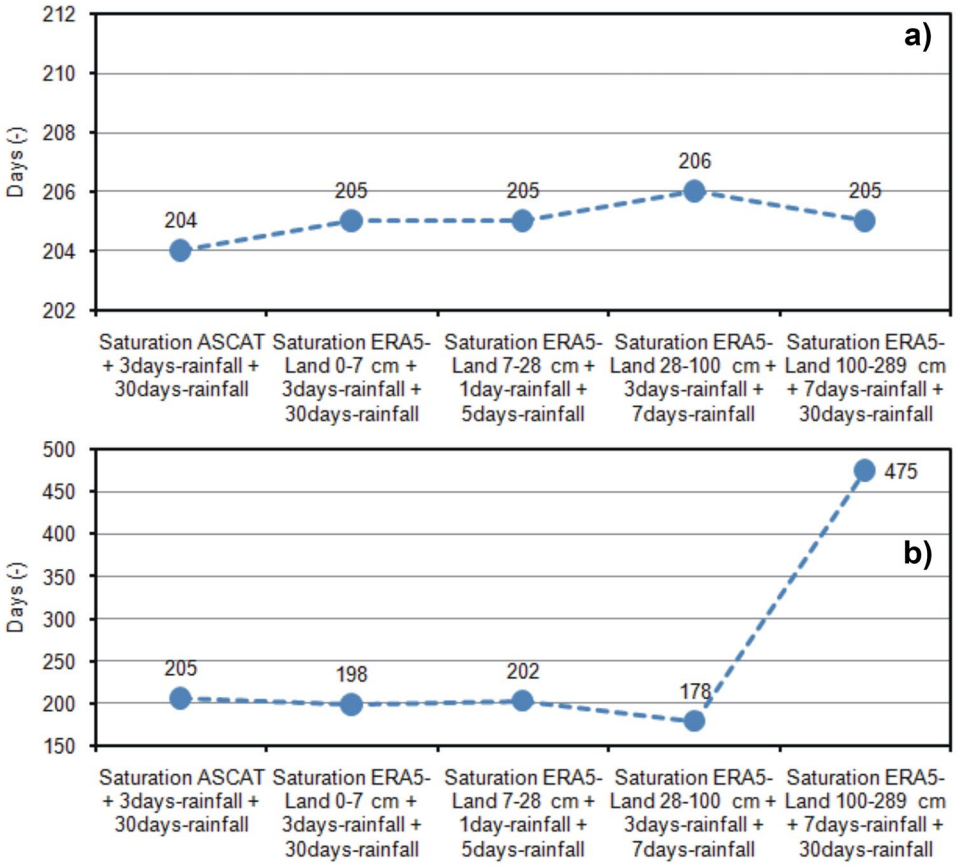

Fig. 8 Number of correctly modeled days with shallow landslide triggering (**a**) and number of days modeled as unstable but without the occurrence of shallow failures (**b**) for the period 2007–2018

a TN of 96.3% and a corresponding FP of 3.7% (Fig. 7b, c). The other models could not obtain similar results since their TN remained lower than 95% and their FP was higher than 5% (Fig. 7b, c). These performances decreased in particular for the model with saturation degree of ERA5-Land 100–289 cm layer, which had TN and FP of only 87.5 and 12.5%, respectively. In terms of days, the most reliable model (saturation degree of ERA5-Land 28–100 cm layer, 3-day rainfall, and 7-day rainfall) within these models overestimated triggering conditions for 178 of 3803 days without the real occurrence of shallow landslides in the input inventory, while the other models overestimated triggering conditions for 198–475 days without real shallow landslides occurrence (Fig. 8b).

Validation of the models

The external validation of the best models was obtained since each type of saturation degree dataset was performed considering the 2019 inventory of triggering and not-triggering days. Sixteen triggering days were detected in November and December 2019, close to the Montuè and Costa Cavalieri test sites. Even if the number of triggering days on the validation year was limited, they could indicate the predictive capabilities of the models considering data not inserted in the model-building procedure. Furthermore, this validation could furnish further indications of the overestimation of the models.

All the selected models, except the one that considered ERA5-Land 100–289 cm saturation degree, estimated triggering conditions correctly on all these days (TP of 100%; Figs. 9a, b and 10a, b). As for the validation of the models through the 2007–2018 inventory, the biggest differences were noted in terms of FP and TN. In these terms, the overestimation of triggering days was lower for the model that considered saturation degree derived from ERA5-Land 28–100 cm, which was able to overestimate only 4 and 9 days at Montuè and Costa Cavalieri, respectively (FP = 1.1–2.5%; Figs. 9c, d and 10c, d).

Figure 11 shows a detailed analysis of the trends of the predictors and the real and modeled triggering and not-triggering days in November–December 2019 for Montuè and Costa Cavalieri test sites, considering the most reliable model (saturation degree of ERA5-Land 28–100 cm layer, 3-day rainfall, and 7-day rainfall). This model identified all the real triggering days correctly at both sites, corresponding to saturation degrees higher than 0.95, 3-day rainfall of 32.2–87.8 mm, and 7-day rainfall of 40.0–135.8 mm. Moreover, the other 12 days, when no shallow failures occurred, were modeled as unstable, representing false positives. This model estimated triggering conditions for these

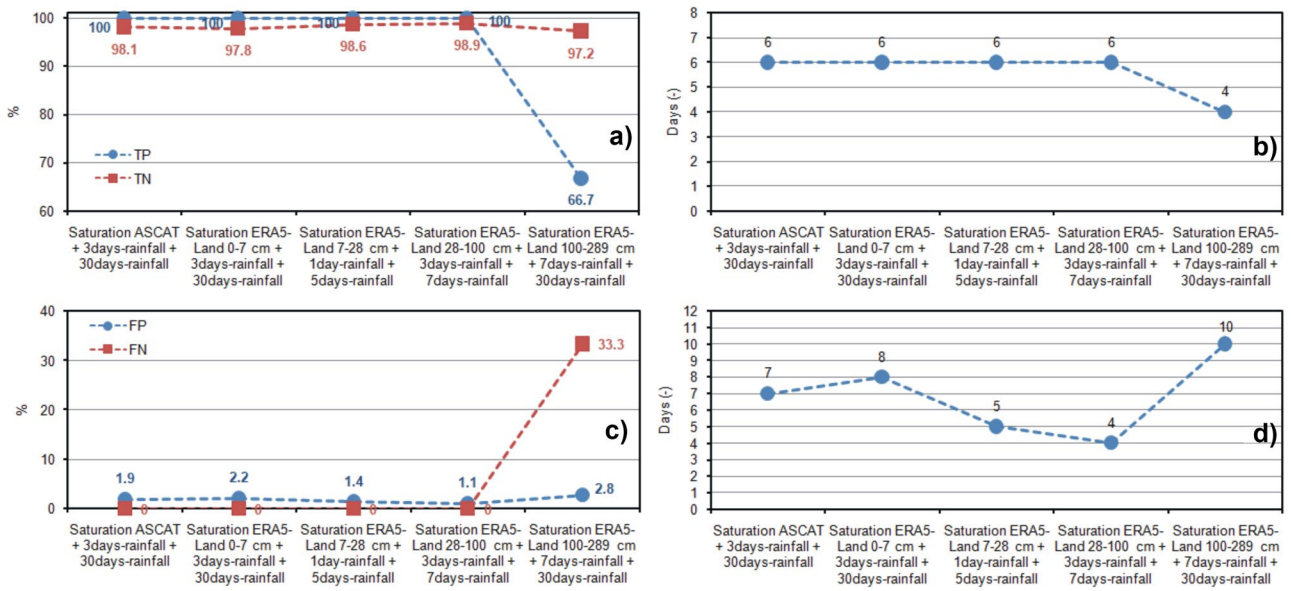

Fig. 9 TP-TN (**a**), number of correctly modeled days with shallow landslide triggering (**b**), FP-FN (**c**), and number of days modeled as unstable but without the occurrence of shallow failures (**d**) for 2019 at Montuè test site

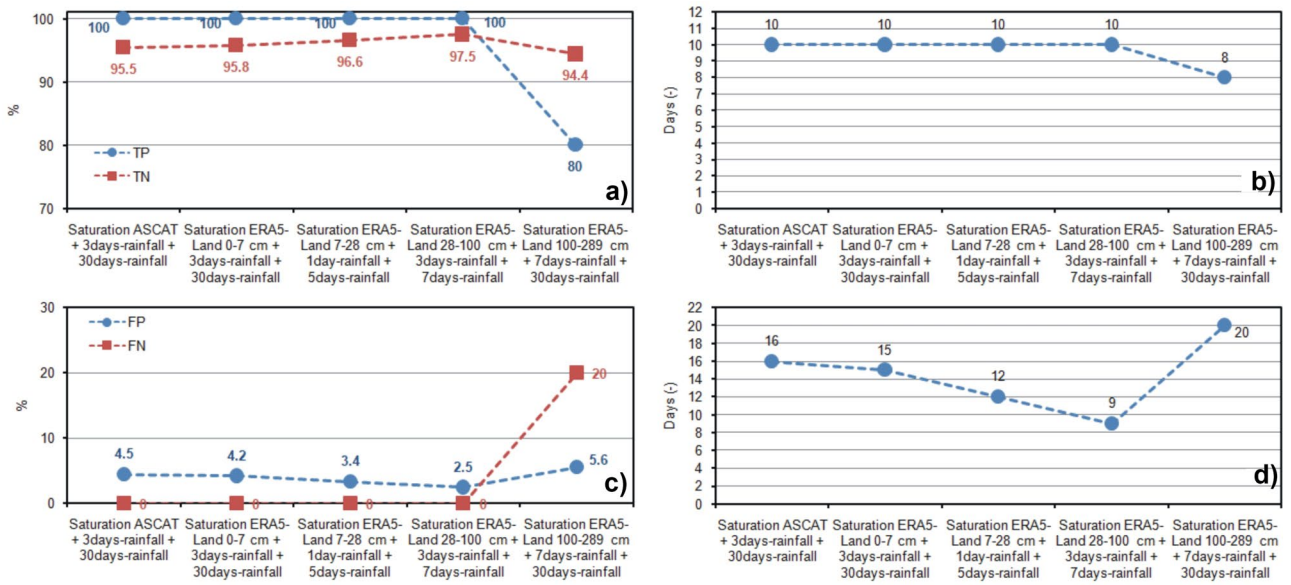

Fig. 10 TP-TN (**a**), number of correctly modeled days with shallow landslide triggering (**b**), FP-FN (**c**), and number of days modeled as unstable but without the occurrence of shallow failures (**d**) for 2019 at Costa Cavalieri test site

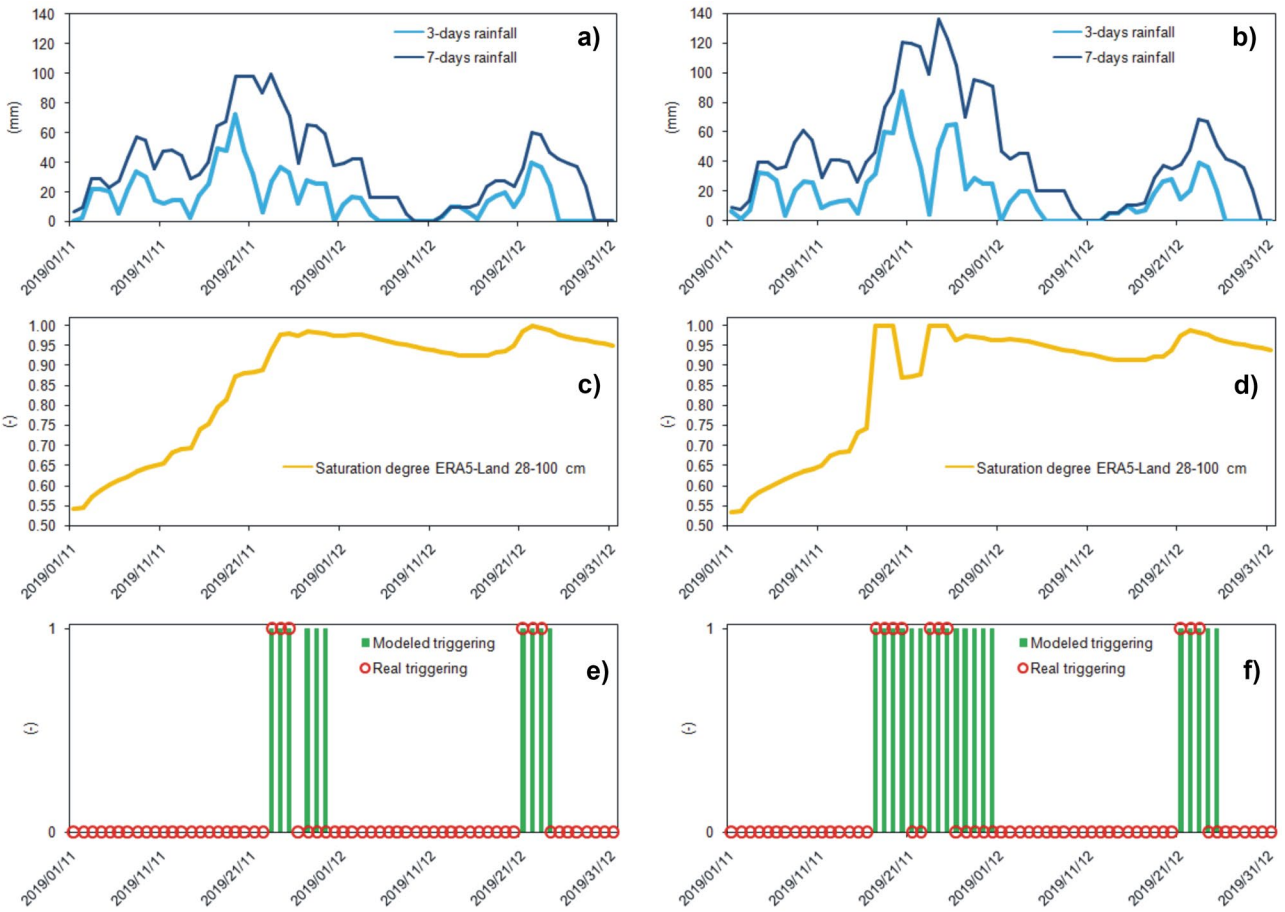

Fig. 11 Three-day and 7-day rainfall at Montuè (**a**) and Costa Cavalieri (**b**), saturation degree estimated since ERA5-Land 28–100 cm at Montuè (**c**) and Costa Cavalieri (**d**), modeled and real triggering days at Montuè (**e**) and Costa Cavalieri (**f**) for the period 1 November–31 December 2019

days when soil saturation was higher than 0.95 and 3-day and 7-day rainfall were over 25.8 and 46.8 mm, respectively.

Hydrological conditions triggering shallow landslides

The best model identified for assessing shallow landslides' temporal probability of occurrence considered the saturation degree of ERA5-Land 28–100 cm layer. In correspondence with shallow landslide triggering days in areas close to Montuè and Costa Cavalieri test sites occurred during their monitoring periods (November 2012–December 2019 at Montuè, March 2016–December 2019 at Costa Cavalieri), saturation degree values measured at the beginning of each triggering day in the field at a depth of the sliding surfaces (0.9–1.0 m from ground level) were compared to the values of saturation degree estimated by ERA5-Land 28–100 cm layer in correspondence of the same days.

As shown in Bordoni et al. (2021b), shallow landslides occurred in geological-geomorphological contexts close to Montuè and Costa Cavalieri when the soil depth, where sliding surfaces developed, was in close-to-saturation conditions at the beginning of a significant rainfall event, characterized by cumulated amounts of at least 30 mm in 3 days. Field measures of saturation degree at the beginning of monitored triggering days confirmed this condition since 13 of 17 triggering days at Montuè and all the 11 triggering days at Costa Cavalieri during the monitoring periods happened for saturation degree higher than 0.95 at the beginning of the triggering rainfall (Fig. 12). Furthermore, the most common values of saturation degree leading to shallow landslides occurrence were 0.99–1.00 at both test sites.

Saturation degree values estimated by the ERA5-Land 28–100 cm layer confirmed these conditions in Montuè and Costa Cavalieri since all the triggering days of the monitoring periods were characterized by saturation degrees higher than 0.95 at both sites (Fig. 12). Moreover, the most common values of saturation degree leading to shallow landslides occurrence were still 0.99–1.00 at both test sites also considering saturation degree retrieved from ERA5-Land 28–100 cm.

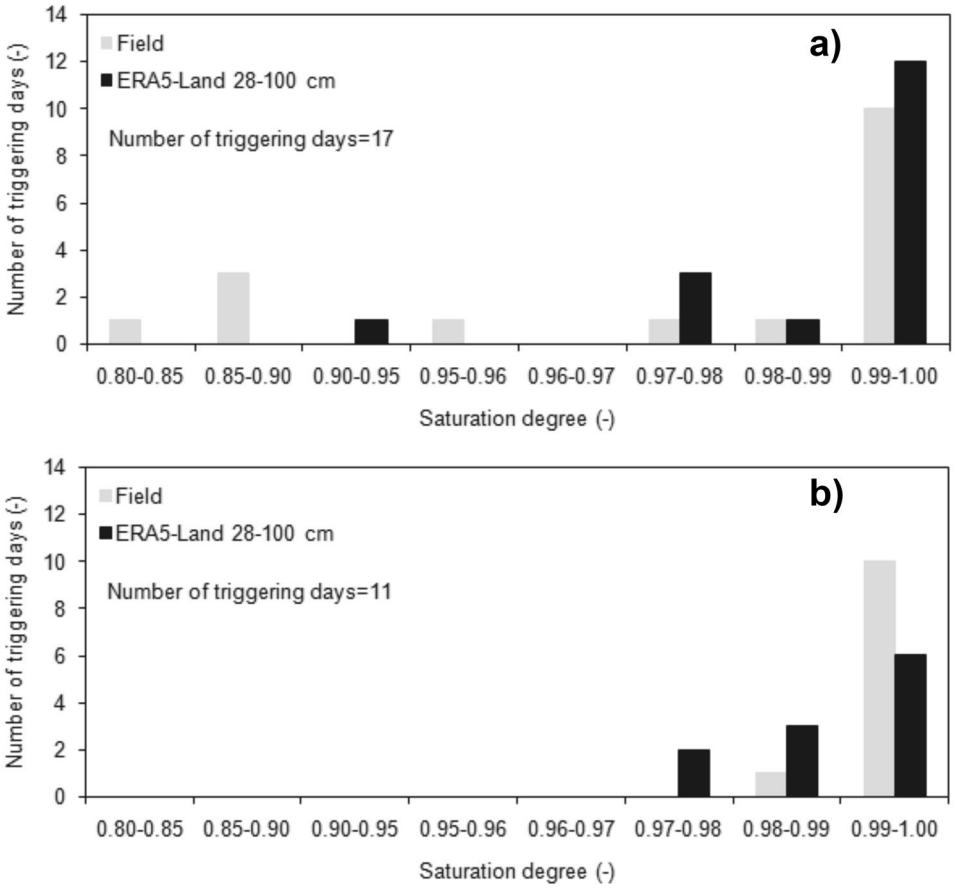

Fig. 12 Saturation degree at 1 m from ground level in correspondence of triggering days at Montuè (**a**) and Costa Cavalieri (**b**) in the period 2007–2019

Discussions

Reliability of ERA5-Land products to reproduce field-measured trend of saturation degree

Evaluating the reliability of soil moisture datasets available by ERA5-Land is fundamental before using these data as input in methods and models for natural hazards assessment, such as landslides. The comparison of ERA5-Land datasets between field-measured time series at different depths represented a robust solution for this assessment and was performed in this study to highlight potential limitations and bias that could influence model predictive capability (Li et al. 2020; Wu et al. 2021).

First, soil moisture datasets derived from the different implemented sources (field, ERA5-Land, ASCAT) were converted into soil saturation time series. Soil saturation trends can help analyze and compare the different hydrological behaviors along a time series (Dente et al. 2012). Saturation degree trends were reconstructed by dividing soil moisture by the saturated water content of each soil horizon, estimated as the highest value of soil moisture measured by each time series. This method of estimating saturated water content can allow obtaining a value of the maximum moisture of soil even if direct measures of saturated water content or porosity are unavailable, improving the possibility of retrieving these products (Li et al. 2020).

In correspondence with the selected test sites, ERA5-Land saturation degree trends can consistently reproduce the different soil hydrological behaviors and processes monitored in the field during dry and wet periods until 1 m in depth, as testified by high values of r and bias indexes (0.77–0.88 for r, 0.08–0.14 for bias), regardless of the different geological and geomorphological features of the selected hillslopes and the physical and hydrological properties of these test sites: clayey-sandy silts of medium–high density (γ of 16.7–18.6 kN/m^3) with low plasticity, high permeability and low water retention properties at Montuè; silty clays of medium–high density (γ of 18.6–19.0 kN/m^3) with high plasticity, high permeability and low water retention properties at Costa Cavalieri.

In the shallowest monitored soil layer up to 0.2 m from the ground, ASCAT products are not in good agreement with real monitored trends since they can capture especially only the long-term hydrological fluctuations related to prolonged periods with consecutive rainfalls or with limited water infiltration and strong evapotranspiration. The agreement between ASCAT and field measures is limited by the

depth of measures of the former sensor. ASCAT allows for retrieval saturation degree of more superficial soil levels (< 10 cm in depth), which could be characterized by a different hydrological dynamic than the one monitored at 0.2 m from the ground (Rotzer et al. 2014). The differences between ASCAT and field trends at 0.2 m from the ground are more evident for saturation measures lower than 0.3 due to more scattered daily trends of ASCAT. Furthermore, the agreement between ASCAT and field trends could also be limited on days with frozen superficial soils and snow cover (Paulik et al. 2014).

The observation on the goodness of ERA5-Land product is in agreement with other comparisons concerning field observations of soil saturation and soil moisture performed in other settings all over the world (Cheng et al. 2019; Mahto and Mishra 2019; Li et al. 2020; Beck et al. 2021; Muñoz-Sabater et al. 2021; Shangguan et al. 2022). The biases are generally correlated with multiple processes between the land and atmosphere that are typically represented less well in models of reanalysis systems, such as soil water transport (Decker and Zeng 2009) and effects of hydraulic non-equilibrium (Vogel et al. 2010).

However, the reliability of ERA5-Land-derived saturation degree is significantly lower in correspondence of soil layers below 1 m from ground level than in the most superficial soil horizons, testified by a decrease in r of 0.18–0.28 and an increase in bias till 0.14 at both the analyzed sites. These discrepancies are again related to processes of water cycles possible in deep soil horizons, which cannot be captured adequately in reanalysis products, in particular exchanges and deep percolation of water between the soil and aquifers (Niu et al. 2007). These differences can also be increased by the physical and hydrological properties of the tested soils, both characterized by high density (γ of 18.2–20.3 kN/m^3), low permeability (K_s of 10^{-7} m/s), and high water retention properties (Wang et al. 2021; Yu et al. 2022).

Estimated saturation degree trends are sensitive to the chosen value of saturated water content. The saturated water content θ_s was considered the highest value of soil moisture measured along the time span for each soil layer. This choice also allowed us to estimate saturation degree conditions on the hypothesis that no field or laboratory estimation of saturated water content or porosity is available. This hypothesis allows retrieving reliable trends of soil saturation degree in both the analyzed contexts, especially until 1 m from the ground, as testified by r (0.77–0.88) and bias (0.08–0.14) values and by the good representation of the real hydrological dynamics in soils. However, local heterogeneities in soil density can also induce heterogeneities in saturated water content and porosity, which will influence the estimation of saturation degree. Table 9 shows the impact on saturation degree due to a possible variation in the saturated water content related to the change in soil density. The higher the decrease in saturated water content, the higher the overestimation of the estimated saturation degree than the one calculated considering the highest measured soil moisture. Instead, an increase in saturated water content value causes an underestimation of the calculated saturation degree, with an increasing trend according to the rise of saturated water content value.

Even if the comparison with field-monitored trends of saturation degree in the analyzed context showed promising results, the implementation of saturation degree trends at different soil depths derived by ERA5-Land products

Table 9 Average overestimation/underestimation on saturation degree according to change in saturated water content values

Saturated water content θ_s (m^3/m^3)/percentage of change in soil density and porosity (%)	Average overestimation/underestimation on saturation degree (%)
Montuè	
0.42/0	-
0.40/ − 5%	+ 4.7
0.38/ − 10%	+ 9.3
0.34/ − 20%	+ 18.6
0.44/ + 5%	− 4.5
0.47/ + 10%	− 8.7
0.50/ + 20%	− 16.0
Costa Cavalieri	
0.45/0	-
0.43/ − 5%	+ 4.3
0.41/ − 10%	+ 8.7
0.38/ − 20%	+ 17.4
0.47/ + 5%	− 4.3
0.49/ + 10%	− 8.2
0.52/ + 20%	− 15.1

for temporal monitoring of soil hydrological processes and for modeling the occurrence of landslides, or other natural hazards as floods or drought (Mahto and Mishra 2019; Shangguan et al. 2022), has to take into account two significant aspects. First, estimating the associated uncertainty on temporal observations of ERA5-Land saturation degree has to be determined, especially if these datasets are used for operational purposes (Munoz-Sabater et al. 2021). Furthermore, data assimilation based on observed saturation degree values data could improve the anomalies concerning field observations and obtain more effective temporal trends at different depths (Zhang et al. 2016; Felsberg et al. 2021).

Use of ERA5-Land products in the model for the temporal assessment of shallow landslides occurrence

The developed methodology for assessing the temporal probability of occurrence of shallow landslides was applied considering different rainfall features and saturation degree trends, derived from ASCAT and ERA5-Land at various soil horizons, for a total of 180 models. For each type of saturation degree product, the developed methodology identified the rainfall parameters that allow the prediction of the days with a high probability of occurrence of shallow landslide triggering with the highest accuracy. According to the type of saturation degree dataset, the rainfall attributes change. However, in all the best models, the rainfall attribute representing the effect of intense and short-term rainfall events is coupled with another rainfall attribute which is a proxy of the long-term effects due to prolonged rainy periods that keep soil in conditions close to complete saturation, causing the decrease of the soil shear strength. This is consistent with the typical rainfall conditions which lead to shallow landslide triggering in the study area, where shallow failures occurred as a consequence of intense rainfalls, characterized by cumulative amounts averagely higher than 30 mm in 3 days, felt on a soil kept in wet conditions by prolonged rainy periods, with rainfall amounts higher than 100 mm in a month, observed mostly from November to April (Bordoni et al. 2021b).

The best models' predictive capability is in the range of outstanding performance. This effectiveness could also be explained by the ability of the chosen data-driven method (MARS), the detection the complex, and, sometimes, nonlinear relationships between rainfall attributes, soil saturation degree, and triggering of shallow landslides (Stanley et al. 2020). Each best model is more sensitive to saturation degree than the other rainfall parameters. Neglecting the saturation degree causes a reduction in the predictive performance of a model, testified by a reduction in AUROC of 0.25–0.32, while AUROC decreases by 0.11–0.17 if one of the rainfall attributes is neglected.

Considering the multi-temporal inventories used as the response variable of the model (2007–2019), all the best models are effective in recognizing the daily occurrence of shallow landslides since they were able to estimate correctly 214–222 days of the 228 triggering days present in the inventories. The model with the highest TP value was the one considering ERA5-Land 28–100 cm layer saturation degree together with 3-day rainfall and 7-day rainfall that missed only 6 days of real triggering events. These days were characterized by complete saturated conditions at that soil layer, but 3-day rainfall lower than 30 mm.

The main difference between these models is recognized in terms of false positives, which represent days modeled as unstable but without the real occurrence of shallow landslides. In these terms, the lower overestimation, represented by the smallest number of false positives, is reached by the model that considers ERA5-Land 28–100 cm layer saturation degree together with 3-day rainfall and 7-day rainfall, which overestimates triggering conditions for only 191 of 4158 days without the real occurrence of shallow landslides, while the other models overestimate triggering conditions for 213–495 days without real shallow landslide triggering. A false positive value of the best model is only 3.7%, i.e., one wrong triggering day about every 30 days, keeping significantly lower than the recommended value of false positive (25%) required for considering an efficient a model for the temporal prediction of slope instabilities (Piciullo et al. 2017). Moreover, even if false positives are still present in all the best models, as also typically observed in other models of the temporal probability of occurrence of slope instabilities as rainfall thresholds (Piciullo et al. 2020), the lowest number of overestimations related to the model that considers saturation degree of the 28–100 cm layer soil layer is consistent with the real depth of sliding surfaces in the study area, located generally in soil levels until 1 m from ground level (Bordoni et al. 2021a, b). Due to the short-term response towards rainfall, conditions of high saturation can be reached more frequently in the most superficial soil horizons, namely, until about 0.3 m from ground level (ASCAT, ERA5-Land 0–7 cm layer, ERA5-Land 7–28 cm layer), providing a bigger number of false positives than underlying soil level that experience high saturation level less frequently (Mirus et al. 2018).

Moreover, saturation degree trends estimated close to the ground level may not truly represent the entire saturation degree profile in depth (Lu and Godt 2013). The huge overestimation of the model with a saturation degree of ERA5-Land 100–289 cm layer can be explained by the permanence of complete saturation or conditions close to saturation in this level for weeks or months during rainy periods. This situation restricts the discrimination of the effects of intense rainfall events leading to triggering conditions (Zhao et al. 2021).

Besides the encouraging and outstanding performances of the best-reconstructed model for the temporal prediction of shallow landslide occurrences, some constraints must be underlined.

First, for applying a similar data-driven approach, a detailed and reliable multi-temporal inventory of past shallow landslide events, indicating the triggering zones and, at least, the days of occurrence, is required (Guzzetti et al. 2012; Corominas et al. 2014).

Regarding the temporal resolution of the used rainfall data, precipitation measured at daily resolution may lead to overestimation in modeling the real hydromechanical response of slopes under rainfall infiltration conditions and, then, in predicting the timing of the occurrence of shallow slope failures (Gariano et al. 2020; Peranic and Arbanas 2022), especially for short rainfall events.

Moreover, even if the model considered ERA5-Land-derived saturation degree, maps of this parameter at a higher resolution should be used, especially in those areas characterized by complex orography or very different land use covers (Dahigamuwa et al. 2018; Felsberg et al. 2021). The use of remotely sensed soil moisture products at higher resolution (Bauer-Marschallinger et al. 2018; Balenzano et al. 2021; Chaudary et al. 2022), downscaling procedures (Wang et al. 2016), and data assimilation systems based on field observations of soil saturation (Girotto et al. 2019; Huang et al. 2021) may improve the estimation of soil hydrological conditions over large and heterogeneous areas.

Another typical constraint is using a reanalysis product, such as ERA5-Land, that adopts atmospheric models. These models are limited by spatial resolution and entailed physical parametrizations and terrain representation, which could affect soil moisture estimation during events developed at a sub-grid scale (e.g., convective precipitation events; Reder and Rianna 2021).

The capability of ERA5-Land products for the identification of hydrological conditions leading to shallow landslides

The best model for assessing shallow landslides' temporal occurrence considered 3-day and 7-day rainfall amounts. Triggering events are modeled for a wide range of these attributes, 19.8–165.0 mm and 61.4–173.2 mm for the 3-day and 7-day rainfall amounts, respectively. The same model considered ERA5-Land 28–100 cm layer saturation degree, which keeps in a lower range than rainfall attributes, especially between 0.76 and 1.00 at the beginning of days of shallow landslide triggering. Saturation degree values derived by ERA5-Land 28–100 cm layer are feasible in identifying triggering days and in comparison with real field values of saturation degree monitored at a depth of sliding surfaces in the selected test sites in the period November 2012–December 2019. This analysis confirms that the ERA5-Land 28–100 cm layer product can be used to correctly estimate conditions close to saturation or saturated conditions (0.80–1.00) measured by field monitoring probes in triggering days, in consequence of intense rainfall events which caused the increase of saturation degree until complete saturation according to a mechanism of upraising of a transient water table since the contact between the most superficial and the deepest soil layers at about 1 m from ground level (Bordoni et al. 2021b).

In these terms, the saturation degree estimated by the ERA5-Land product at the layer where the shallow landslides' sliding surfaces typically form in the study area (28–100 cm layer) represents an important parameter for detecting soil hydrological conditions leading to shallow landslides, reducing the biases of the predictions based only on rainfall information. In particular, it allows representing the hydrological response of the soil towards intense rainfalls according to different initial soil water statuses, providing a fundamental tool to discriminate similar rainfall amounts able to trigger or not shallow landslides according to the high value of soil saturation (Bordoni et al. 2021a; Reder and Rianna 2021; Zhao et al. 2021).

Conclusions

This study exploited the use of saturation degree derived from ERA5-Land datasets of different soil layer depths for the temporal prediction of shallow landslides occurrence and for the correct identification of soil hydrological conditions which could lead to the triggering, considering as test site a representative area of northern Italian Apennines significantly prone to these phenomena.

The following outcomes can be summarized:

1. ERA5-Land-derived saturation degree trends well estimate the field-monitored datasets acquired in different contexts of the study area, especially until 1 m from ground level and for the different hydrological conditions;
2. ERA5-Land-derived saturation degree can represent a significant predictor of a data-driven method for estimating the temporal probability of occurrence of shallow landslides. The best model considers, in particular, saturation degree trends in the 28–100 cm layer, consistent with the typical depths of shallow failures sliding surfaces in the study area. Considering the saturation degree of this layer in the model reduces the overestimation of triggering respect to models with saturation degrees of more superficial or deeper levels;
3. The saturation degree estimated by the ERA5-Land product of the 28–100 cm layer allows the detection of

soil hydrological conditions leading to shallow landslides in the study area, reducing the biases of the predictions based only on rainfall predictors.

In conclusion, the ERA5-Land-derived saturation degree of the layer where shallow landslides typically form has a greater potential to be used for identifying the hydrological conditions leading to shallow landsliding in the study area, enhancing the predictive capability of methods using datasets of near-surface or deeper information. This parameter is also a fundamental and dynamic predisposing factor for the right prediction of triggering or not-triggering conditions of shallow landslides. Furthermore, ERA5-Land saturation degree trends could be useful for other hydrological applications also in agricultural contexts of sloping terrains (e.g., vineyards, sowed fields).

As ERA5 data are freely available and constantly updated in near real time (delay of 5 days behind real time), derived, saturation degree values could be easily implemented to improve the effectiveness of early warning systems based only on rainfall attributes, helping in the identification of soil hydrological attributes potentially leading to shallow slope failures. Moreover, they can be adapted to identify triggering conditions and to develop prediction methods in areas with scarce field data, operating as a fundamental tool for increasing the management of landslides hazard and the resilience of those territories. The flexibility and feasibility of the method make it potentially applicable to different geological and geomorphological settings. Other study cases are needed to have a clear frame about the correct estimation of real field saturation degree trends and the support to shallow landslides prediction provided by ERA5-Land products.

Acknowledgements ERA5-Land data have been generated using Copernicus Climate Change Service Information and downloaded from the Copernicus Climate Change Service Climate Data Store: https://cds.climate.copernicus.eu/cdsapp#!/dataset/reanalysis-era5-land?tab=form. We also thank the anonymous reviewers for their revisions and suggestions.

Funding Open access funding provided by Università degli Studi di Pavia within the CRUI-CARE Agreement. This work has been in the frame of the ANDROMEDA project, which has been supported by Fondazione Cariplo, grant no. 2017–0677, and of the VIRECLI project, which has been supported by Regione Lombardia.

Data availability Data are available on request from the authors.

References

Abraham MT, Satyam N, Rosi A, Pradhan B, Segoni S (2021) Usage of antecedent soil moisture for improving the performance of rainfall thresholds for landslide early warning. Catena 105147. https://doi.org/10.1016/j.catena.2021.105147

Aleotti P (2004) A warning system for rainfall-induced shallow failures. EngGeol 73:247–265. https://doi.org/10.1016/j.enggeo.2004.01.007

Balenzano A, Satalino FMG, Lovergine FP, Palmisano D, Peng J, Marzahn P, Wegmüller U, Cartus O, Dąbrowska-Zielińska K, Musial JP, Davidson MWJ, Pauwels VRN, Cosh MH, McNairn H, Johnson JT, Walker JP, Yueh SH, Entekhabi D, Kerr YH, Jackson TJ (2021) Sentinel-1 soil moisture at 1 km resolution: a validation study. Remote Sens Environ 263:112554. https://doi.org/10.1016/j.rse.2021.112554

Bauer-Marschallinger B, Paulik C, Hochstöger S, Mistelbauer T, Modanesi S, Ciabatta L, Massari C, Brocca L, Wagner W (2018) Soil moisture from fusion of scatterometer and SAR: closing the scale gap with temporal filtering. Remote Sens 10(7):1030. https://doi.org/10.3390/rs10071030

Beck HE, Pan M, Miralles DG, Reichle RH, DorigoWA HS, Sheffield J, Karthikeyan L, Balsamo G, Parinussa RM, van Dijk AIJM, Du J, Kimball JS, Vergopolan N, Wood EF (2021) Evaluation of 18 satellite- and model-based soil moisture products using in situ measurements from 826 sensors. Hydrol Earth Syst Sci 25:17–40. https://doi.org/10.5194/hess-25-17-2021

Bordoni M, Corradini B, Lucchelli L, Valentino R, Bittelli M, Vivaldi V, Meisina C (2019) Empirical and physically based thresholds for the occurrence of shallow landslides in a prone area of northern Italian Apennines. Water 11:2653. https://doi.org/10.3390/w11122653

Bordoni M, Vivaldi V, Lucchelli L et al (2021a) Development of a data-driven model for spatial and temporal shallow landslide probability of occurrence at catchment scale. Landslides 18:1209–1229. https://doi.org/10.1007/s10346-020-01592-3

Bordoni M, Bittelli M, Valentino R, Vivaldi V, Meisina C (2021b) Observations on soil-atmosphere interactions after long-term monitoring at two sample sites subjected to shallow landslides. Bull Eng Geol Environ 80:7467–7491. https://doi.org/10.1007/s10064-021-02334-y

Brocca L, Melone F, Moramarco T (2008) On the estimation of antecedent wetness condition in rainfall–runoff modeling. Hydrol Process 22:629–642. https://doi.org/10.1002/hyp.6629

Brocca L, Ponziani F, Moramarco T, Melone F, Berni N, Wagner W (2012) Improving landslide forecasting using ASCAT-derived soil moisture data: a case study of the Torgiovannetto landslide in central Italy. Remote Sens 4(5):1232–1244. https://doi.org/10.3390/rs4051232

Brunetti MT, Peruccacci S, Rossi M, Luciani S, Valigi D, Guzzetti F (2010) Rainfall thresholds for the possible occurrence of landslides in Italy. Nat Hazards Earth Syst Sci 10:447–458. https://doi.org/10.5194/nhess-10-447-2010

Brunetti MT, Melillo M, Peruccacci S, Ciabatta L, Brocca L (2018) How far are we from the use of satellite rainfall products in landslide forecasting? Remote Sens Environ 210:65–75. https://doi.org/10.1016/j.rse.2018.03.016

Chaudary SK, Srivastava PK, Gupta DK, Kumar P, Prasad R, Pandey DK, Das AK, Gupta M (2022) Machine learning algorithms for soil moisture estimation using Sentinel-1: model development and

implementation. Adv Space Res 69(4):1799–1812. https://doi.org/10.1016/j.asr.2021.08.022
Cheng M, Zhong L, Ma Y, Zou M, Ge N, Wang X, Hu Y (2019) Soil moisture products and reanalysis data for the Tibetan Plateau. Remote Sens 11:1196. https://doi.org/10.3390/rs11101196
Conrad JL, Morphew MD, Baum RL (2021) Mirus BB (2021) HydroMet: a new code for automated objective optimization of Hydrometeorological Thresholds for Landslide Initiation. Water 13:1752. https://doi.org/10.3390/w13131752
Corominas J, Van Westen C, Frattini P, Cascini L, Malet JP, Fotopoulou S, Catani F, Van Den Eeckhaut M, Mavrouli O, Agliardi F, Pitilakis K, Winter MG, Pastor M, Ferlisi S, Tofani V, Hervas J (2014) Smith JT (2014) Recommendations for the quantitative analysis of landslide risk. Bull EngGeolEnviron 73:209–263. https://doi.org/10.1007/s10064-013-0538-8
Cruden DM Varnes DJ (1996) Landslide types and processes. In: Turner AK, Schuster RL (eds) Landslides: investigation and mitigation. National Academy Press, Washington, D.C., pp 36–75
Dahigamuwa T, Gunaratne M, Li M (2018) An improved data-driven approach for the prediction of rainfall-triggered soil slides using downscaled remotely sensed soil moisture. Geosciences 8:326. https://doi.org/10.3390/geosciences8090326
Decker M, Zeng XB (2009) Impact of modified Richards equation on global soil moisture simulation in the community land model (CLM3.5). J Adv Model Earth Systems 1:22. https://doi.org/10.3894/James.2009.1.5
Dente L, Vekerdy Z, Wen J, Su Z (2012) Maqu network for validation of satellite-derived soil moisture products. Int J Appl Earth Obs 17:55–65. https://doi.org/10.1016/j.jag.2011.11.004
Felsberg A, De Lannoy GJM, Girotto M, Poesen J, Reichle RH, Stanley T (2021) Global soil water estimates as landslide predictor: the effectiveness of SMOS, SMAP, and GRACE observations, land surface simulations, and data assimilation. J Hydrometeorol 22:1065–1084. https://doi.org/10.1175/JHM-D-20-0228.1
Friedman JH (1991) Multivariate adaptive regression splines. Ann Stat 19:1–141. http://www.jstor.org/stable/2241837. Accessed 4 April 2022
Fusco F, DeVita P, Mirus BB, Baum RL, Allocca V, Tufano R, Di Clemente E, Calcaterra D (2019) Physically based estimation of rainfall thresholds triggering shallow landslides in volcanic slopes of southern Italy. Water 11:1915. https://doi.org/10.3390/w11091915
Galanti Y, Barsanti M, Cevasco A, D'Amato Avanzi G, Giannecchini R (2018) Comparison of statistical methods and multi-time validation for the determination of the shallow landslide rainfall thresholds. Landslides 15:937–952. https://doi.org/10.1007/s10346-017-0919-3
Gariano SL, Melillo M, Peruccacci S, Brunetti MT (2020) How much does the rainfall temporal resolution affect rainfall thresholds for landslide triggering? Nat Hazards 100:655–670. https://doi.org/10.1007/s11069-019-03830-x
Giannecchini R, Galanti Y, D'Amato Avanzi G (2012) Critical rainfall thresholds for triggering shallow landslides in the Serchio River Valley (Tuscany, Italy). Nat Hazards Earth Syst Sci 12:829–842. https://doi.org/10.5194/nhess-12-829-2012
Girotto MG, Reichle RH, Rodell M, Liu Q, Mahanama S, De Lannoy GJM (2019) Multi-sensor assimilation of SMOS brightness temperature and GRACE terrestrial water storage observations for soil moisture and shallow groundwater estimation. Remote SensEnviron 227:12–27. https://doi.org/10.1016/j.rse.2019.04.001
Guzzetti F, Peruccacci S, Rossi M, Stark CP (2008) The rainfall intensity-duration control of shallow landslides and debris flows: an update. Landslides 5:3–17. https://doi.org/10.1007/10346-007-0112-1
Guzzetti F, Mondini AC, Cardinali M, Fiorucci F, Santangelo M, Chang K-T (2012) Landslide inventory maps: new tools for an old problem. Earth Sci Rev 112:42–66. https://doi.org/10.1016/j.earscirev.2012.02.001
Guzzetti F, Gariano SL, Peruccacci S, Brunetti MT, Marchesini I, Rossi M, Melillo M (2020) Geographical landslide early warning systems. Earth Sci Rev 200:102973. https://doi.org/10.1016/j.earscirev.2019.102973
Hersbach H, Dee D (2016) ERA5 reanalysis is in production. ECMWF Newsletter No 147:7
Hersbach H, Bell B, Berrisford P, Hirahara S, Horányi A, Muñoz-Sabater J, Nicolas J, Peubey C, Radu R, Schepers D, Simmons A, Soci C, Abdalla S, Abellan X, Balsamo G, Bechtold P, Biavati G, Bidlot J, Bonavita M, Chiara G, Dahlgren P, Dee D, Diamantakis M, Dragani R, Flemming J, Forbes R, Fuentes M, Geer A, Haimberger L, Healy S, Hogan RJ, Hólm E, Janisková M, Keeley S, Laloyaux P, Lopez P, Lupu C, Radnoti G, Rosnay P, Rozum I, Vamborg F, Villaume S, Thépaut JN (2020) The ERA5 global reanalysis. Quar J Royal Meteorol Soc 146(730):1999–2049. https://doi.org/10.1002/qj.3803
Hosmer DW, Lemeshow S (2000) Applied logistic regression. Wiley, New York
Huang M, Crawford JH, DiGangi JP, Carmichael GR, Bowman KW, Kumar SV, Zhan X (2021) Satellite soil moisture data assimilation impacts on modeling weather variables and ozone in the southeastern US – Part 1: an overview. Atmos Chem Phys 21:11013–11040. https://doi.org/10.5194/acp-21-11013-2021
Ji L, Senay GB, Verdin JP (2015) Evaluation of the Global Land Data Assimilation System (GLDAS) air temperature data products. J Hydrometeorol 16:2463–2480. https://doi.org/10.1175/JHM-D-14-0230.1
Kim SW, Chun KW, Kim M, Catani F, Choi B, Seo JI (2020) Effect of antecedent rainfall conditions and their variations on shallow landslide-triggering rainfall thresholds in South Korea. Landslides. https://doi.org/10.1007/s10346-020-01505-4
Kim H, Lee J-H, Park H-J, Heo J-H (2021) Assessment of temporal probability for rainfall-induced landslides based on nonstationary extreme value analysis. EngGeol 294:106372. https://doi.org/10.1016/j.enggeo.2021.106372
Lacasse S, Nadim F, Kalsnes B (2010) Living with landslide risk. Geotech Eng J Seags Agssea 41:1–13
Lee J-H, Kim H, Park H-J, Heo J-H (2021) Temporal prediction modeling for rainfall-induced shallow landslide hazards using extreme value distribution. Landslides 18:321–338. https://doi.org/10.1007/s10346-020-01502-7
Leonarduzzi E, McArdell BW, Molnar P (2021) Rainfall-induced shallow landslides and soil wetness: comparison of physically based and probabilistic predictions. Hydrol Earth Syst Sci 25:5937–5950. https://doi.org/10.5194/hess-25-5937-2021
Li M, Wu P, Ma Z (2020) A comprehensive evaluation of soil moisture and soil temperature from third-generation atmospheric and land reanalysis data sets. Int J Climatol 40:5744–5766. https://doi.org/10.1002/joc.6549
Liu Y, Yang Y (2022) Advances in the quality of global soil moisture products: a review. Remote Sens 14:3741. https://doi.org/10.3390/rs14153741
Lu N, Godt JW (2013) Hillslope hydrology and stability. Cambridge University Press, New York
Mahto SS, Mishra V (2019) Does ERA-5 outperform other reanalysis products for hydrologic applications in India? J Geophys Res Atm 124:9423–9441. https://doi.org/10.1029/2019JD031155
Malardel S, Wedi N, Deconinck W, Diamantakis M, Kuehnlein C, Mozdzynski G, Hamrud M, Smolarkiewicz P (2016) A new grid for the IFS. ECMWF Newsletter 146:23–28. https://doi.org/10.21957/zwdu9u5i
Meisina C (2004) Swelling-shrinking properties of weathered clayey soils associated with shallow landslides. Quat J Eng Geol Hydrogeol 37:77–94. https://doi.org/10.1144/1470-9236/03-044

Meisina C (2006) Characterisation of weathered clayey soils responsible for shallow landslides. Nat Hazards Earth Syst Sci 6:825–838. https://doi.org/10.5194/nhess-6-825-2006

Mirus BB, Becker RE, Baum RL, Smith JB (2018) Integrating real-time subsurface hydrologic monitoring with empirical rainfall thresholds to improve landslide early warning. Landslides 15:1909–1919. https://doi.org/10.1007/s10346-018-0995-z

Munoz-Sabater J, Dutra E, Agustí-Panareda A, Albergel C, Arduini G, Balsamo G, Boussetta S, Choulga M, Harrigan S, Hersbach H, Martens B, Miralles DG, Piles M, Rodríguez-Fernández NJ, Zsoter E, Buontempo C, Thépaut J-N (2021) ERA5-Land: a state-of-the-art global reanalysis dataset for land applications. Earth Syst Sci Data 13:4349–4383. https://doi.org/10.5194/essd-13-4349-2021

Niu GY, Yang ZL, Dickinson RE, Gulden LE, Su H (2007) Development of a simple groundwater model for use in climate models and evaluation with gravity recovery and climate experiment data. J Geophys ResAtm 112(D7):1–12. https://doi.org/10.1029/2006jd007522

Palazzolo N, Peres DJ, Creaco E, Cancelliere A (2022) Potential improvements of landslide prediction by hydro-meteorological thresholds: an investigation based on reanalysis soil moisture data and principal component analysis, Nat Hazards Earth Syst Sci Discuss [preprint]. https://doi.org/10.5194/nhess-2022-175

Pan J, Shangguan W, Li L, Yuan H, Zhang S, Lu X, Wei N, Dai Y (2019) Using data-driven methods to explore the predictability of surface soil moisture with FLUXNET site data. Hydrol Process 33:2978–2996. https://doi.org/10.1002/hyp.13540

Park J-Y, Lee S-R, Lee D-H, Kim Y-T, Lee J-S (2019) A regional-scale landslide early warning methodology applying statistical and physically based approaches in sequence. Eng Geol 260:105193. https://doi.org/10.1016/j.enggeo.2019.105193

Paulik C, Dorigo W, Wagner W, Kidd R (2014) Validation of the ASCAT Soil Water Index using in situ data from the International Soil Moisture Network. Int J App Earth Obs Geoinf 30:1–8. https://doi.org/10.1016/j.jag.2014.01.007

Peranic J, Arbanas Z (2022) The influence of the rainfall data temporal resolution on the results of numerical modelling of landslide reactivation in flysch slope. Landslides 19:2809–2822. https://doi.org/10.1007/s10346-022-01937-0

Picarelli L, Olivares L, Damiano E, Darban R, Santo A (2020) The effects of extreme precipitations on landslide hazard in the pyroclastic deposits of Campania Region: a review. Landslides 17:2343–2358. https://doi.org/10.1007/s10346-020-01423-5

Piciullo L, Dahl M-P, Devoli G, Colleuille H, Calvello M (2017) Adaptation of the EDuMaP method for the performance evaluation of the alerts issued on variable warning zones. Nat Hazards Earth Sys 17(6):817–831. https://doi.org/10.5194/nhess-17-817-2017

Piciullo L, Tiranti D, Pecoraro G, Cepeda JM, Calvello M (2020) Standards for the performance assessment of territorial landslide early warning systems. Landslides 17:2533–2546. https://doi.org/10.1007/s10346-020-01486-4

Piciullo L, Gilbert G (2020) Definition of soil water content and rainfall thresholds for landslide occurrence. EGU General Assembly 2020 (EGU2020-16688), updated on 3 April 2022. https://doi.org/10.5194/egusphere-egu2020-16688

Ponziani F, Pandolfo C, Stelluti M, Berni N, Brocca L, Moramarco T (2012) Assessment of rainfall thresholds and soil moisture modeling for operational hydrogeological risk prevention in the Umbria region (central Italy). Landslides 9(2):229–237. https://doi.org/10.1007/s10346-011-0287-3

Reder A, Rianna G (2021) Exploring ERA5 reanalysis potentialities for supporting landslide investigations: a test case from Campania Region (Southern Italy). Landslides 18:1909–1924. https://doi.org/10.1007/s10346-020-01610-4

Rodell M, Houser P, Jambor U, Gottschalck J, Mitchell K, Meng C-J, Arsenault K, Cosgrove B, Radakovich J, Bosilovich M (2004) The global land data assimilation system. Bull Am Meteorol Soc 85:381–394. https://doi.org/10.1175/BAMS-85-3-381

Rosi A, Segoni S, Canavesi V, Monni A, Gallucci A, Casagli N (2021) Definition of 3D rainfall thresholds to increase operative landslide early warning system performances. Landslides 18:1045–1057. https://doi.org/10.1007/s10346-020-01523-2

Rotzer K, Montzka C, Bogena H, Wagner W, Kerr YH, Kidd R, Vereecken H (2014) Catchment scale validation of SMOS and ASCAT soil moisture products using hydrological modeling and temporal stability analysis. J Hydrol 519A:934–946. https://doi.org/10.1016/j.jhydrol.2014.07.065

Salciarini D, Fanelli G, Tamagnini C (2017) A probabilistic model for rainfall-induced shallow landslide prediction at the regional scale. Landslides 14:1731–1746. https://doi.org/10.1007/s10346-017-0812-0

Seneviratne SI, Koster RD, Guo Z, Dirmeyer PA, Kowalczyk E, Lawrence D, Liu P, Mocko D, Lu C-H, Oleson KW, Verseghy D (2006) Soil moisture memory in AGCM simulations: analysis of global land–atmosphere coupling experiment (glace) data. J Hydrometeor 7(5):1090–1112. https://doi.org/10.1175/Jhm533.1

Shangguan W, Zhang R, Li L, Zhang S, Zhang Y, Huang F, Li J, LiuW, (2022) Assessment of agricultural drought based on reanalysis soil moisture in Southern China. Land 11:502. https://doi.org/10.3390/land11040502

Stanley TA, Kirschbaum DB, Sobieszczyk S, Jasinski M, Borak J, Slaughter S (2020) Building a landslide hazard indicator with machine learning and land surface models. Environ Model Software 129:104692. https://doi.org/10.1016/j.envsoft.2020.104692

Tien Bui D, Pradhan B, Lofman O, Revhaug I, Dick OB (2013) Regional prediction of landslide hazard using probability analysis of intense rainfall in the HoaBinh province. Vietnam Nat Hazards 66(2):707–730. https://doi.org/10.1007/s11069-012-0510-0

Uwihirwe J, Riveros A, Wanjala H, Schellekens J, Sperna Weiland F, Hrachowitz M, Bogaard TA (2022) Potential of satellite-derived hydro-meteorological information for landslide hazard assessment thresholds in Rwanda, EGUsphere [preprint], https://doi.org/10.5194/egusphere-2022-596

Van Genuchten MT (1980) A closed-form equation for predicting the hydraulic conductivity of unsaturated soils. Soil Sci Soc Am J 44:892–898. https://doi.org/10.2136/sssaj1980.03615995004400050002x

Vasu NN, Lee SR, Pradhan AMS, Kim YT, Kang SH, Lee DH (2016) A new approach to temporal modelling for landslide hazard assessment using an extreme rainfall induced-landslide index. EngGeol 215:36–49. https://doi.org/10.1016/j.enggeo.2016.10.006

Vogel HJ, Weller U, Ippisch O (2010) Non-equilibrium in soil hydraulic modelling. J Hydrol 393:20–28. https://doi.org/10.1016/j.jhydrol.2010.03.018

Wagner W, Hahn S, Kidd R, Melzer T, Bartalis Z, Hasenauer S, Figa-Saldaña J, de Rosnay P, Jann A, Schneider S, Komma J, Kubu G, Brugger K, Aubrecht C, Züger J, Gangkofner U, Kienberger S, Brocca L, Wang Y, Blöschl G, Eitzinger J, Steinnocher K (2013) The ASCAT soil moisture product: a review of its specifications, validation results, and emerging applications. MeteorologischeZeitschrift 22:5–33

Wang J, Ling Z, Wang Y, Zeng H (2016) Improving spatial representation of soil moisture by integration of microwave observations and the temperature-vegetation-drought index derived from MODIS products. ISPRS J Photogramm Remote Sens 113:144–154. https://doi.org/10.1016/j.isprsjprs.2016.01.009

Wang X, Chen D, Pang G et al (2021) Effects of cumulus parameterization and land-surface hydrology schemes on Tibetan Plateau climate simulation during the wet season: insights from the

RegCM4 model. Clim Dyn 57:1853–1879. https://doi.org/10.1007/s00382-021-05781-1

Wu Z, Feng H, He H, Zhou J, Zhang Y (2021) Evaluation of soil moisture climatology and anomaly components derived from ERA5-Land and GLDAS-2.1 in China. Water Resour Manag 35:629–643. https://doi.org/10.1007/s11269-020-02743-w

Yang K-H, Nguyen TS, Rahardjo H, Lin D-G (2021) Deformation characteristics of unstable shallow slopes triggered by rainfall infiltration. Bull Eng Geol Environ 80:317–344. https://doi.org/10.1007/s10064-020-01942-4

Yu J, Zheng W, Xu L, Meng F, Li J, Zhangzhong L (2022) TPE-CatBoost: an adaptive model for soil moisture spatial estimation in the main maize-producing areas of China with multiple environment covariates. J Hydrol 613B:128465. https://doi.org/10.1016/j.jhydrol.2022.128465

Zezere JL, Vaz T, Pereira S, Oliveira SC, Marques R, Garcia R (2015) Rainfall thresholds for landslide activity in Portugal: a state of art. Environ Earth Sci 73:2907–2936. https://doi.org/10.1007/s12665-014-3672-0

Zhang D, Madsen H, Ridler ME, Kidmose J, Jensen KH (2016) Refsgaard JC (2016) Multivariate hydrological data assimilation of soil moisture and groundwater head. Hydrol Earth Syst Sci 20:4341–4357. https://doi.org/10.5194/hess-20-4341-2016

Zhao B, Dai Q, Zhou L, Zhu S, Shen Q, Han D (2021) Assessing the potential of different satellite soil moisture products in landslide hazard assessment. Remote Sens Environ 264:112583. https://doi.org/10.1016/j.rse.2021.112583